NeuroImage: Clinical 45 (2025) 103760

Contents lists available at ScienceDirect

NeuroImage: Clinical

journal homepage: www.elsevier.com/locate/ynicl

Event-related potential markers of subjective cognitive decline and mild cognitive impairment during a sustained visuo-attentive task

A.A. Vergani [a,b], S. Mazzeo [d,f,g], V. Moschini [d], R. Burali [e], M. Lassi [a,b], L.G. Amato [a,b], J. Carpaneto [a,b], G. Salvestrini [e], C. Fabbiani [c,e], G. Giacomucci [c,d], C. Morinelli [d], F. Emiliani [c], M. Scarpino [e], S. Bagnoli [c], A. Ingannato [c], B. Nacmias [c,e], S. Padiglioni [d], S. Sorbi [c,d,e], V. Bessi [c,d,*], A. Grippo [e], A. Mazzoni [a,b]

[a] The BioRobotics Institute, Sant'Anna School of Advanced Studies, viale Rinaldo Piaggio 34, 56025 Pontedera-Pisa, Italy
[b] Department of Excellence in Robotics and AI, Sant'Anna School of Advanced Studies, viale Rinaldo Piaggio 34, 56025 Pontedera-Pisa, Italy
[c] Department of Neuroscience, Psychology, Drug Research and Child Health, Azienda Ospedaliero-Universitaria Careggi, Largo Brambilla 3, Florence 50134, Italy
[d] Research and Innovation Centre for Dementia-CRIDEM, Azienda Ospedaliero-Universitaria Careggi, Largo Brambilla 3, Florence 50134, Italy
[e] IRCCS Fondazione Don Carlo Gnocchi, via di Scandicci, 269, 50143 Florence, Italy
[f] Vita-Salute San Raffaele University, Via Olgettina, 58, 20132 Milano, Italy
[g] IRCCS Policlinico San Donato, Piazza Edmondo Malan, 2, 20097 San Donato Milanese, Italy

ARTICLE INFO

Keywords:
Subjective Cognitive Decline (SCD)
Mild Cognitive Impairment (MCI)
EEG
Event-related potentials

ABSTRACT

Subjective cognitive decline (SCD), mild cognitive impairment (MCI), and Alzheimer's disease stages lack well-defined electrophysiological correlates, creating a critical gap in the identification of robust biomarkers for early diagnosis and intervention. In this study, we analysed event-related potentials (ERPs) recorded during a sustained visual attention task in a cohort of 178 individuals (119 SCD, 40 MCI, and 19 healthy subjects, HS) to investigate sensory and cognitive processing alterations associated with these conditions. SCD patients exhibited significant attenuation in both sensory (P1, N1, P2) and cognitive (P300, P600, P900) components compared to HS, with cognitive components showing performance-related gains. In contrast, MCI patients did not show a further decrease in any ERP component compared to SCD. Instead, they exhibited compensatory enhancements, reversing the downward trend observed in SCD. This compensation resulted in a non-monotonic pattern of ERP alterations across clinical conditions, suggesting that MCI patients engage neural mechanisms to counterbalance sensory and cognitive deficits. These findings support the use of electrophysiological markers in support of medical decision-making, enhancing personalized prognosis and guiding targeted interventions in cognitive decline.

1. Introduction

Neurocognitive disorders affect 6–50 million people worldwide, with prevalence doubling every five years, particularly among those aged 50–80. This trend poses a significant societal burden, with various factors contributing to dementia, including neurological, systemic, and psychiatric conditions. Alzheimer's disease (AD) is the most prevalent cause of neurocognitive decline (Livingston et al., 2020). AD involves the accumulation of beta-amyloid plaques and neurofibrillary tangles, leading to neurodegeneration and cognitive decline, eventually resulting in dementia. This process unfolds over decades, with amyloid buildup occurring years before symptoms. Stages range from subtle cognitive changes to full-blown dementia. The initial stage, Subjective Cognitive Decline (SCD), involves self-reported cognitive decline while performance on standardized tests remains within the normal range when adjusted for age, sex, and education (Jessen et al., 2014; Jessen et al., 2020). Mild Cognitive Impairment (MCI) occurs when pathological scores on neuropsychological tests are present without a significant impact on daily life activities. It serves as a transitional stage between normal aging and the more severe cognitive decline seen in dementia (Gauthier et al., 2006). In the realm of dementia research, SCD and MCI hold paramount significance as they fall within the spectrum of AD

* Corresponding author at: Department of Neuroscience, Psychology, Drug Research and Child Health, University of Florence, AOU Careggi, Largo Brambilla 3, Florence 50134, Italy.
E-mail address: valentina.bessi@unifi.it (V. Bessi).

https://doi.org/10.1016/j.nicl.2025.103760
Received 16 July 2024; Received in revised form 11 February 2025; Accepted 16 February 2025
Available online 25 February 2025

(Jessen et al., 2014; Jessen et al., 2020; Slot et al., 2019; Rabin et al., 2015). Patients affected by these conditions present an opportunity for intervention with recently developed Disease-Modifying Therapies (DMTs) approved for AD (van Dyck et al., 2023; Budd Haeberlein et al., 2022). Indeed, it is widely acknowledged that DMTs should be administered during the early stages of the disease, prior to the onset of neurodegeneration (Guest et al., 2022).

Seeking reliable biomarkers for early AD diagnosis is crucial. Common biomarkers like MRI, FDG-PET, and CSF are invasive and not widely available. Hence, researchers explore accessible options, with EEG showing promise (Rossini et al., 2022). Nevertheless, despite these efforts, only a limited number of studies have delved into this promising avenue (e.g., biomarking conditions as SCD and MCI (Alexander et al., 2006; Babiloni et al., 2010; Ganapathi et al., 2022; Che et al., 2024; Wang et al., 2024; Xiao et al., 2022), MCI against AD (Paitel et al., 2021), across CSF (Smailovic et al., 2018) and ApoE ε-4 allele (Cintra et al., 2018).

Additionally, in dementia EEG studies, sensory event-related potentials are examined (e.g., auditory (Morrison et al., 2018) and visual (Harding et al., 1985; Kolev et al., 2002; Karamacoska et al., 2019; Saito et al., 2001). Specifically, visual event-related potentials suggest a compelling hypothesis about brain alterations in the visual system that could help detect early structural changes linked to anomalies in ERPs (Chapman and Bragdon, 1964; Armstrong, 2009; Javitt et al., 2023). For example, by recording EEG during a visuo-memory task, Waninger et al (Waninger et al., 2018) found amplitude suppression of late positive potentials (~400 ms) in MCI against healthy subjects over right occipital and temporal channels. Other studies enquired early phase of visual processing as the encoding of stimulus: Krasodomska et al (Krasodomska et al., 2010) found N95 wave dynamics alterations in AD, as other colleagues in last decays detect visual evoked potential anomalies in dementia patients (Pollock et al., 1989; Mangun, 1995). Hence, an unresolved critical aspect is how visual alterations manifest across various stages of cognitive decline.

Along with the early visual alterations associated with cognitive decline, abnormalities of the late post-stimulus ERP components related to the quality of decision-making are known. Among the best studied is the P300, which is altered in gain or latency in pathological conditions such as AD dementia (Hedges et al., 2016; Polich et al., 1986; Braverman et al., 2006; van Deursen et al., 2009; Jiang et al., 2015; Parra et al., 2012), as well as for the P600, which has been observed that its abnormalities are associated with increased risk of conversion to dementia in MCI patients (Olichney et al., 2008; Olichney et al., 2013; Dröge et al., 2016; Kimiskidis and Papaliagkas, 2012; Gu and Zhang, 2017; Morrison et al., 2019; Amariglio et al., 2012).

Following the hypothesis that visual faculties play a key role in uncovering electrophysiological abnormalities associated with cognitive decline, we conducted an exploratory study using a visual-attentive experimental paradigm while recording cortical EEG activity during task execution. To this end, we first assessed the behavioral outcomes of individuals with SCD and MCI, comparing them with healthy subjects (HS). However, behavioral assessments alone may not fully capture the neurobiological alterations underlying cognitive decline.

To bridge this gap, biomarker-based ERPs provide a crucial neural criterion where cognitive testing alone may fall short. While SCD represents an earlier stage of impairment compared to MCI, it may already conceal significant neurobiological alterations that only direct neural measurements can reveal (Jessen et al., 2014; Jessen et al., 2020; Valles-Salgado et al., 2024; Perrotin et al., 2012; van Harten et al., 2013; Hendriksen et al., 2024; Liu et al., 2024; Mazzeo et al., 2024; Hong et al., 2023; Stern, 2009), that are alterations that could eventually lead to MCI or even AD. The discrepancy between neural data and cognitive performance can often be attributed to brain resilience (Stern, 2006; Stern et al., 2023; Barulli and Stern, 2013; Stern et al., 2003; Argiris et al., 2024; Argiris et al., 2023; Vockert et al., 2024; Hasanzadeh et al., 2025; Katayama et al., 2024), which may obscure or compensate for underlying neurodegenerative pathology. In this context, electrophysiological markers derived from ERPs serve as invaluable tools for detecting latent pathological changes (Balart-Sánchez et al., 2024; Buss et al., 2023; Devos et al., 2023; Quinzi et al., 2020; Speer and Soldan, 2015; Habeck et al., 2003; Mazzeo et al., 2023) and providing a more comprehensive understanding of disease progression. These neural markers are therefore essential in detecting hidden brain alterations, refining our understanding of cognitive decline.

We aimed to establish ERP correlates as biomarkers of underlying AD pathology along the cognitive decline continuum. By examining task performance as an indicator of cognitive function, we wanted to explore how neural recruitment is associated with behavioral outcomes and how this modulation varies with disease progression from SCD to MCI.

2. Methods

2.1. Clinical protocol

The clinical protocol of the PREVIEW project (ClinicalTrials.gov Identifier: NCT05569083) has been published previously (Jessen et al., 2014). In brief, PREVIEW is a longitudinal study on Subjective Cognitive Decline started in October 2020 with the aim to identify features derived from easily accessible, cost-effective and non-invasive assessment to accurately detect SCD patients who will progress to AD dementia. All participants were collected in agree with the Declaration of Helsinki and with the ethical standards of the Committee on Human Experimentation of Careggi University Hospital (Florence, Italy). The study was approved by the local Institutional Review Board (reference 15691oss).

2.2. Participants

We enrolled 178 individuals (117F), including 119 SCD patients (85F), 40 MCI patients (24F), and 19 healthy individuals (8F). All participants underwent thorough family and clinical history evaluations, neurological examinations, extensive neuropsychological assessments, premorbid intelligence estimation, and depression evaluations.

Patients underwent an extensive neuropsychological examination (see specific references in (Jessen et al., 2014), including global measurements (MMSE), attention (Trial Making Test A/B and BA, visual search), and premorbid intelligence estimation (TIB). Personality traits (Big Five Factors Questionnaire − BFFQ), and leisure activities evaluation (structured interviewed regarding participation in intellectual, sporting and social activities).

The following inclusion criteria were adopted: satisfied criteria for SCD (Albert et al., 2011) or MCI (McKhann et al., 2011); Mini Mental State Examination (MMSE) score > 24, corrected for age and education; normal functioning on the Activities of Daily Living (ADL) and the Instrumental Activities of Daily Living (IADL) scales unsatisfied criteria for AD diagnosis according to National Institute on Aging-Alzheimer's Association (NIA-AA) criteria (Alcolea et al., 2019). Exclusion criteria were history of head injury, current neurological and/or systemic disease, symptoms of psychosis, major depression, substance use disorder; complete data loss of patients' follow-up; use of any medication with known effects on EEG oscillations, such as benzodiazepines or antiepileptic drugs.

A subset of 58 patients (34 SCD and 24 MCI) underwent CSF collection for assessment of $A\beta_{42}$, $A\beta_{42}/A\beta_{40}$, total-tau (t-tau) and phosphorylated-tau (p-tau). Among these, 31 patients also underwent cerebral amyloid-PET. Normal values for CSF biomarkers were: $A\beta_{42} >$ 670 pg/ml, $A\beta_{42}/A\beta_{40}$ ratio > 0.062, t-tau < 400 pg/ml and p-tau < 60 pg/ml (Giacomucci et al., 2021). Methods used CSF collection, biomarker analysis, and amyloid-PET acquisition and rating are described in further detail elsewhere (Jessen et al., 2014; Jack et al., 2016). Patients who underwent AD biomarker assessment, were classified as A + if at least one of the amyloid biomarkers (CSF $A\beta_{42}$, $A\beta_{42}/A\beta_{40}$ or amyloid PET) indicated the presence of Aβ pathology, and as A-

if none of the biomarkers indicated the presence of Aβ pathology. In cases where there were conflicting results between CSF and Amyloid PET, only the pathological result was considered. Patients were classified as T + or T- based on whether their CSF p-tau concentrations were higher or lower than the cut-off value, respectively. Similarly, patients were classified as N + or N- depending on whether their t-tau concentrations were higher or lower than the cut-off value. Using this initial classification, we applied the NIA-AA Research Framework (Stikic et al., 2011) to define the following groups: ATN Negative (46 of 58; 29 SCD of 34 + 17 MCI of 24): normal AD biomarkers (A-/T-/N-) and ATN Positive (12 of 58; 5 SCD + 7 MCI): pathological AD biomarkers (if at least A or T or N were+).

2.3. Visuo-attentive task

The visuo-attentive experimental paradigm chosen is the 3-Choice Vigilance Test (3-CVT) requires identifying a target shape (upward triangle) among two distractor shapes (downward triangle and diamond) (Krasodomska et al., 2010). Shapes are shown for 0.2 s with varied interstimulus intervals in the 20-minute task. Participants press left for targets (70 %) and right for distractors (30 %). Performance is evaluated using reaction time, accuracy, and F-Measure, that is a combined metric that integrates processing reaction time and accuracy ensuring a balanced assessment that prevents misleading interpretations (see equations in (Danjou et al., 2019).

2.4. EEG devices

EEG data were collected from eligible subjects at IRCCS Don Gnocchi (Florence, Italy) using the 64-channel Galileo-NT system (E.B. Neuro S. p.a.). Sensor placement followed the extended 10/20 system (Delorme and Makeig, 2004). Signals were recorded unipolarly at 512 Hz. Electrode impedances were maintained between 7 and 10 KOhm; if exceeded, electrodes were readjusted, and affected segments were removed.

2.5. EEG preprocessing and ERP component definition

EEG processing included band-pass filtering (1–45 Hz), noisy channel interpolation, average re-referencing, and artefactual component exclusion via ICA (Siems et al., 2016). Trials lasted 1000 ms, with 200 ms for stimulus presentation and 800 ms for response (participants had in average 421.32 trials (std = 77.57)). ERPs were epoch-aligned with correct responses to the target stimulus, segmented from 0 to 1000 ms with a −100 ms baseline. Average EEG signals from occipital and central channels (FC1, FCz, FC2, C1, Cz, C2) were computed for encoding and decision-making analysis, respectively. In the stimulus encoding phase, particular interest was shown in the P1, N1 and P2 components, while in the decision phase, the components of greatest interest were P300, P600 and P900. The name of component is based on the sign of the potential (e.g., "P" for positive and "N" for negative) and the latency of the peak at which they are expected to appear (the case of cognitive components, e.g., P300) or the order (the case of sensorial components, e.g., the 1st positive is P1).

2.6. Neural features computations

We extracted neural features from defined ERP components, including voltage peaks, latencies, and integrals (Simpson method) from each channel of occipital and central scalp parcellations. The computation of the integration time window was performed once the peak of the components was identified, with the width of the window proportional to the extent of the component. The features of these components were extracted using a custom-developed algorithm that identifies peaks, latencies, and integrals within a predefined time window. We also introduced an occipital-seed based functional connectivity metrics with the aim to evaluate the amount of similarity between seed channels and other channels of the scalp. We chose the time series recorded from occipital channels (PO7, PO8, O1, Oz, O2) as the seed and examined their relationship with other scalp channels. This approach is justified by the nature of our experimental task, which involves visuospatial attention, making it reasonable to investigate scalp-wide covariation relative to occipital regions. The similarity measure adopted is the Spearman rank-order correlation coefficient (Spearman, 1961; Tan et al., 2016; Dukart et al., 2011) computed within encoding (0–200 ms) timeframe. We then counted the channels that had correlations with ($p < 0.05$) and ($r > 0.90$) and computed the percentage relative to the total number of channels. This measurement allowed us to assess the extent of extra-seed recruitment of channels (the more the channels are similar to the occipital seed, the more they are engaged with the occipital seed, the more are the neural sources used during encoding process). A value close to 0 % indicated that no channel was highly correlated with the occipital seed, while a value greater than 0 % indicated the extent of extra-seed recruitment.

2.7. Statistical analysis

Non-parametric analysis was employed, with statistics presented as mean values and std (where possible). Pair and group analysis were done with Kruskal-Wallis H test. Statistical differences in ERP voltage dynamics were assessed instant-by-instant by computing H statistics on voltage values at considered groups: i.e., for each instant t and group g we first compute the matrices $[v_g]_t^{c\times n}$, where v_g is the set of voltage values of a given group g, $c \times n$ is the matrix dimension of c (number of channels) and n (number of subjects within the group g); then, we statistically compared each group matrix as an empirical distribution of voltage values. The multiple comparison correction used for ERP dynamics was the FDR Benjamini-Hochberg, while for all the other test was Bonferroni. Data preprocessing utilized EEGLAB (Siems et al., 2016), while postprocessing and visualization were performed using Python libraries (numpy, scipy, pandas). To account for the effect of age on neural features and task performance, we applied an age correction procedure using a linear model (Pukelsheim, 1994). Specifically, we employed the Huber Regressor (sklearn.linear_model.HuberRegressor) to regress each neural feature against age and subsequently removed the age-related variance. Scripts of pre and postprocessing are available at https://github.com/albertoarturovergani/PREVIEWTCVT.

2.8. Outliers management

All 178 participants performed the 3-CVT task. Poor behavioural performance was not ground for exclusion, as we aimed to reflect the variability encountered in real-world applications. Instead, we applied an exclusion criterion based on neural features extracted from ERP dynamics: participants who exceeded the 3-sigma cut-off (Luck et al., 1994) for at least two neural features were excluded. This led to the exclusion of 2 MCI and 4 SCD patients.

2.9. Visual summary

A summary of the results and methodologies implemented can be seen in Fig. 1. Cognitive decline followed a monotonically decreasing course with age and the speed of the loss of mental faculties depended on the presence of a cognitive pathology such as SCD, MCI or severe forms of dementia such as AD (Fig. 1A). Task performance also followed a monotonically decreasing course in line with the severity of the clinical condition (Fig. 1B). Simultaneous recording of the EEG signal during task performance (Fig. 1C) captured the dynamics of occipital and central ERP components distinct for clinical conditions (Fig. 1D). The components distinguished significantly for their dynamics across clinical conditions were the occipital P1 and N1 components and the central components (P300, P600, P900). Feature extraction from the identified

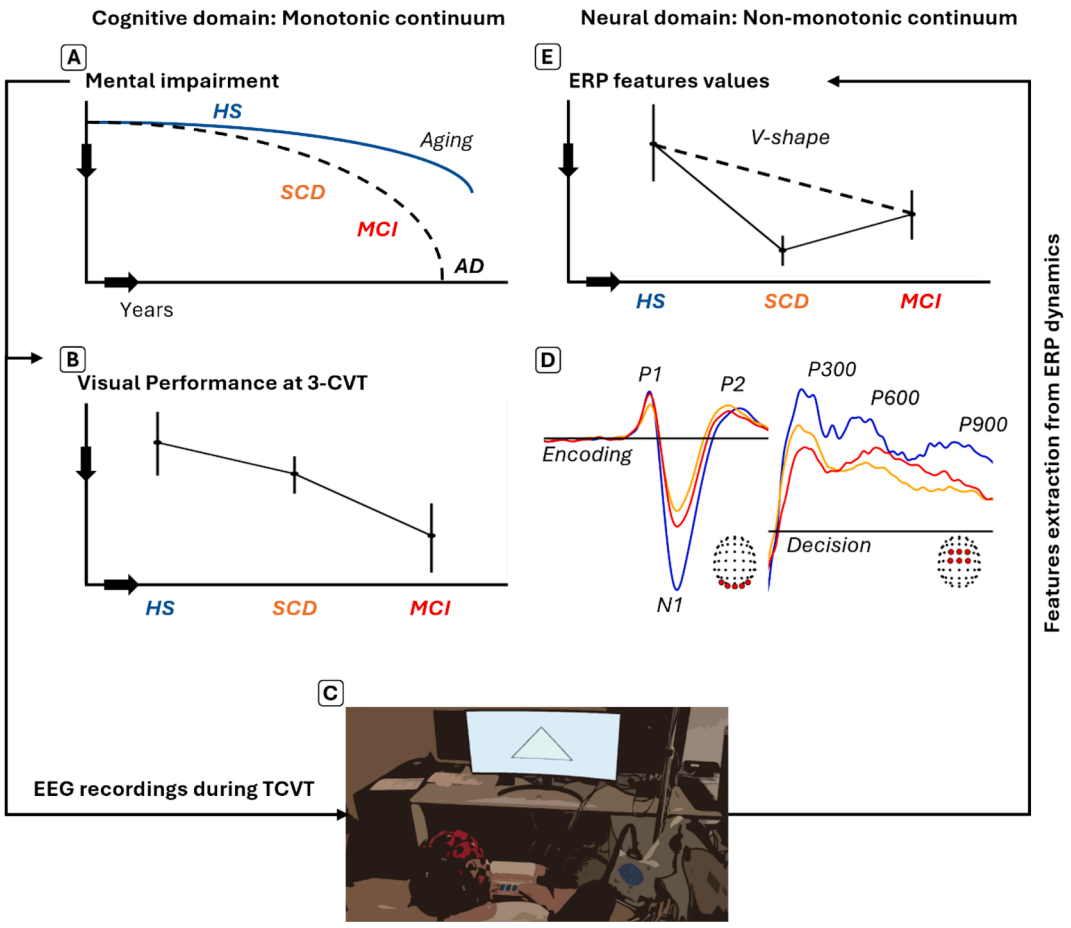

Fig. 1. Visual abstract. (A) Monotonic decreasing relationship between age and cognitive decline, modulated in its course by the presence of SCD or MCI pathology (or eventually AD). Dashed line traces the pathological deviation from healthy path line. (B) Performance on the visuo-attentive task 3-CVT following a monotonic decreasing course according to the severity of the pathology. (C) Experimental EEG signal recording setting while participants were performing the 3-CVT task. (D) ERP dynamics extracted from occipital and central channels separated by clinical condition, where occipital channels probed the encoding phase of the stimulus, and the central channels probed the decision-making phase of the stimulus. (E) Non-monotonic (V-shape) trend of ERP features reflecting increased recruitment of neural resources by MCI patients. Dashed line traces the hypothetical monotonic trend which has been altered by the features values.

components revealed a non-monotonic trend in their values, showing MCIs to have a greater recruitment of neural resources (Fig. 1E).

3. Results

3.1. Participant profiling

The multidimensional profile indicated that individuals with SCD and MCI differed significantly on several clinical, psychological and behavioural scales (see group statistics in Table 1). Patients with MCI had a higher age, lower educational level and lower performance on cognitive and visuomotor assessments than subjects with SCD and HS. Subjects with SCD demonstrated higher levels of intellectual and social activity than those with MCI and were more likely to have a family history of Alzheimer's disease. HS subjects, on the other hand, were only examined on a few scales, showed the highest scores on cognitive tests (e.g. MMSE), were younger and had the highest levels of education compared to both SCD and MCI groups. Overall, the HS subjects showed better cognitive functioning and better education levels, highlighting their status as a reference or control group in this study.

3.2. Task performance at 3CVT

Despite a trend across behavioural measures followed cognitive decline, only accuracy exhibited statistically significant differences among the groups. The F-Measure did not show significant differences ($H = 4.26$, $p = 0.12$; Table 1), and post-hoc analyses confirmed no significant pairwise differences among HS vs. SCD ($H = 0.401$, $p = 1.000$), SCD vs. MCI ($H = 3.320$, $p = 0.205$), and HS vs. MCI ($H = 2.929$, $p = 0.261$) (Fig. 2A). Similarly, reaction time was not significantly different across groups ($H = 0.32$, $p = 0.85$; Table 1), with post-hoc analyses indicating comparable reaction times among HS vs. SCD ($H = 0.260$, $p = 1.000$), SCD vs. MCI ($H = 1.576e\text{-}05$, $p = 1.000$), and HS vs. MCI ($H = 0.380$, $p = 1.000$) (Fig. 2B). In contrast, accuracy showed a significant group effect ($H = 6.53$, $p = 0.04$; Table 1). Post-hoc analyses revealed that this difference was primarily driven by a significant contrast between SCD and MCI ($H = 5.921$, $p = 0.044$), with MCI participants performing significantly worse than those with SCD. However, no significant differences were found between HS and SCD ($H = 0.059$, $p = 1.000$) or HS and MCI ($H = 3.572$, $p = 0.176$) (Fig. 2C). These results indicate that, although accuracy varied across clinical conditions, some MCI patients achieved accuracy levels comparable to HS. This finding supports the classification of participants into low and high performance groups based on median accuracy. This dichotomous division enables further investigation of ERP neural markers in relation to performance levels (see Section 3.5).

3.3. Clinical conditions have specific ERP dynamics

The analysis of ERP dynamics revealed condition-specific patterns in

Table 1
Demographic, clinical characteristics and task performance of study participants.

Class	Scale	HS (n = 19)	SCD (n = 119)	MCI (n = 40	p(H)
Task	F-Measure [a.u.]	0.92 (0.03)	0.91 (0.04)	0.90 (0.05)	0.12 (4.26)
Task	Accuracy [%]	93.59 (3.23)	92.96 (4.70)	90.01 (7.28)	*0.04 (6.53)
Task	Reaction time [s]	0.47 (0.08)	0.48 (0.08)	0.48 (0.09)	0.85 (0.32)
Clinical	MMSE [a.u.]	29.15 (1.09)	27.51 (2.14)	26.39 (2.40)	**0.00 (18.73)
Clinical	Education [years]	14.95 (3.32)	13.41 (3.65)	10.32 (3.88)	***0.00 (23.73)
Clinical	Age [years]	62.53 (5.08)	65.40 (9.23)	72.75 (8.37)	***0.00 (23.79)
Clinical	TIB [a.u]	– (–)	113.33 (3.60)	110.62 (6.38)	0.56 (4.66)
Clinical	Age at onset [years]	– (–)	56.98 (9.03)	63.30 (10.06)	**0.01 (12.85)
Clinical	Family history of AD [count]	– (–)	74 (–)	25 (–)	0.11 (12.85)
Visuo-attentive	Trail Making Test B-A [a.u.]	– (–)	33.35 (35.47)	115.21 (177.39)	*0.02 (10.69)
Visuo-attentive	Trail Making Test A [a.u.]	– (–)	29.62 (14.37)	40.48 (39.89)	1.00 (2.67)
Visuo-attentive	Trail Making Test A [a.u.]	– (–)	63.08 (43.91)	155.72 (190.79)	*0.02 (10.37)
Visuo-attentive	Attentive matrices [a.u.]	– (–)	51.00 (6.45)	47.81 (7.93)	0.16 (6.85)
Leasure time	Intellectual activity [a.u.]	– (–)	18.87 (3.38)	16.99 (5.32)	0.19 (6.51)
Leasure time	Social activity [a.u.]	– (–)	9.04 (2.80)	8.08 (2.69)	0.86 (3.92)
Leasure time	Sport activity [a.u.]	– (–)	6.53 (2.48)	6.03 (2.27)	1.00 (0.54)
Psychological	Extraversion [a.u.]	– (–)	45.76 (5.51)	44.38 (5.97)	0.94 (3.78)
Psychological	Agreableness [a.u.]	– (–)	50.83 (7.59)	48.40 (6.38)	0.06 (8.63)
Psychological	Coscientiousness [a.u.]	– (–)	49.89 (7.67)	49.00 (7.01)	1.00 (0.44)
Psychological	Emotive stability [a.u.]	– (–)	50.20 (7.08)	49.25 (6.91)	1.00 (2.01)
Psychological	Openness of mind [a.u.]	– (–)	46.11 (6.25)	42.73 (6.07)	0.09 (7.95)

Note. The table is organized into scales divided by category: clinical, leisure time, psychological (Big Five), visual-attentive, and task performance. The values represent the mean and standard deviation (SD) for each scale across three groups: Subjective Cognitive Decline (SCD, N = 119), Mild Cognitive Impairment (MCI, N = 40), and Healthy Subjects (HS, N = 19). Pairwise comparisons use the Kruskal-Wallis test, with p-values (p(H)) associated with the H-statistic. Significant p-values are marked with asterisks: * ($p < 0.05$), ** ($p < 0.01$), *** ($p < 0.001$), **** ($p < 0.0001$).

the potential amplitudes. In the occipital channels, statistically significant temporal differences ($p < 0.05$) were observed between clinical conditions (Fig. 3A), particularly for the P1 (54–82 ms; HS > SCD for 57.14 % of the time, MCI > SCD for 100 %) and N1 (93–195 ms; HS < MCI for 75.51 % of the time, HS < SCD for 100 % of the time, MCI < SCD for 59.18 % of the time) components. Interestingly, the temporal dynamics of P1 and N1 amplitudes were not monotonically related to condition severity. Instead, greater attenuation of P1 and N1 amplitude profiles was observed in SCD compared to both MCI and HS. In the central channels, significant differences in instantaneous amplitudes were identified between clinical conditions (Fig. 3B) for the P300/600/900 components ($p < 0.05$; >335 ms). These components were generally attenuated in patients compared to HS, with HS > MCI for 64.41 % of the time, HS > SCD for 90.59 % of the time, and MCI ≠ SCD for 41.47 % of the time. Notably, for the P600, MCI demonstrated an amplified gain compared to SCD, suggesting distinct dynamics in later cognitive processing stages across conditions.

The feature extraction (Table 2) process revealed distinct differences in ERP dynamics across the three groups. For latency, P2 showed significant differences between SCD and HS, with HS exhibiting longer latencies. Similarly, N1 latency was higher in HS compared to SCD. P900 latency displayed a significant difference between SCD and MCI, with SCD showing higher values. For peak amplitude, N1 and P600 demonstrated strong significance in comparisons involving HS. Specifically, N1 peak was higher in HS compared to both SCD and MCI. P600 peak was significantly higher in HS compared to SCD, with moderate differences observed between SCD and MCI. For integral values, several features exhibited consistent significance. P2 and N1 integrals were higher in HS compared to SCD and MCI. P600 and P900 integrals also displayed significant differences, with higher values observed in HS compared to SCD and MCI. These results indicated that HS consistently exhibited stronger and more pronounced ERP responses across multiple features compared to SCD and MCI. Overall, the table highlighted how ERP dynamics differed among the three groups, with HS showing stronger neural responses, particularly for features like N1 and P600. Moreover, correlation analysis (S-Fig. 1) of ERP latency versus peak amplitude for components across groups showed significant correlations for P1 in all groups and for P300 in SCD and MCI. Other components (P2, N1, P600, P900) did not exhibit significant correlations, except for a trend in P900 for MCI.

The results presented in this section concern participants who had and had not undergone the CSF examination. However, if only CSF patients are considered, distinguishing between SCD and MCI, similar temporal trends can be observed, which means that the peak order of potential for N1, P300 and P900 is preserved (S-Fig. 2). Subsequent analyses will continue to consider all patients.

3.4. ERP features follow a non-monotonic ordering showing attenuation for SCD and amplification for MCI

Previous analyses suggested that electrophysiological correlates of clinical conditions followed a non-monotonic pattern, where ERP features did not progress linearly with the severity of cognitive pathology. To investigate the contribution of feature types (latency, peak, and integral) to this non-monotonic trend, feature values were normalized relative to HS participants and expressed as percentage deviations (Fig. 4). The normalized latency (Fig. 4A) showed no significant differences between groups (HS vs. SCD: $H = 3.642$, $p = 0.169$; SCD vs. MCI: $H = 0.025$, $p = 1.000$; HS vs. MCI: $H = 2.602$, $p = 0.320$). This indicated that latency remained stable across clinical groups. In contrast, the normalized peak (Fig. 4B) displayed significant differences between HS and SCD ($H = 10.31$, $p = 0.0039$) and HS and MCI ($H = 5.846$, $p = 0.0468$), while no significant differences were found between SCD and MCI ($H = 0.454$, $p = 1.000$). The normalized integral (Fig. 4C) exhibited the strongest differences, following a non-monotonic pattern (HS > SCD < MCI). Significant differences were observed between HS and SCD ($H = 25.95$, $p < 0.0001$) and HS and MCI ($H = 9.747$, $p = 0.0053$), with a trend between SCD and MCI ($H = 5.197$, $p = 0.0678$). Overall, SCD showed a greater percentage reduction in integrals (−30.74 %) compared to MCI (–22.37 %) relative to healthy subjects (HS), indicating a more pronounced decline in the early stages of cognitive impairment (Fig. 4C and Fig. 5A/B/C). These findings highlighted that while latency remained stable, peak and integral features were more sensitive to clinical conditions, with the integral showing the strongest non-monotonic trend.

We expanded the aggregated integrals (Fig. 4C) to examine the percentage variations in ERP potential across clinical conditions. In the comparison between SCD and HS (Fig. 5A), significant reductions were observed in the integrals of N1 (−44.62 %) and P2 (−30.61 %). These results indicate that N1 and P2 represent the primary markers of alteration in SCD compared to HS, highlighting marked changes already in the early stages of cognitive decline. In the comparison between MCI and HS (Fig. 5B), the integrals of N1 (−34.21 %) and P2 (−21.29 %) showed

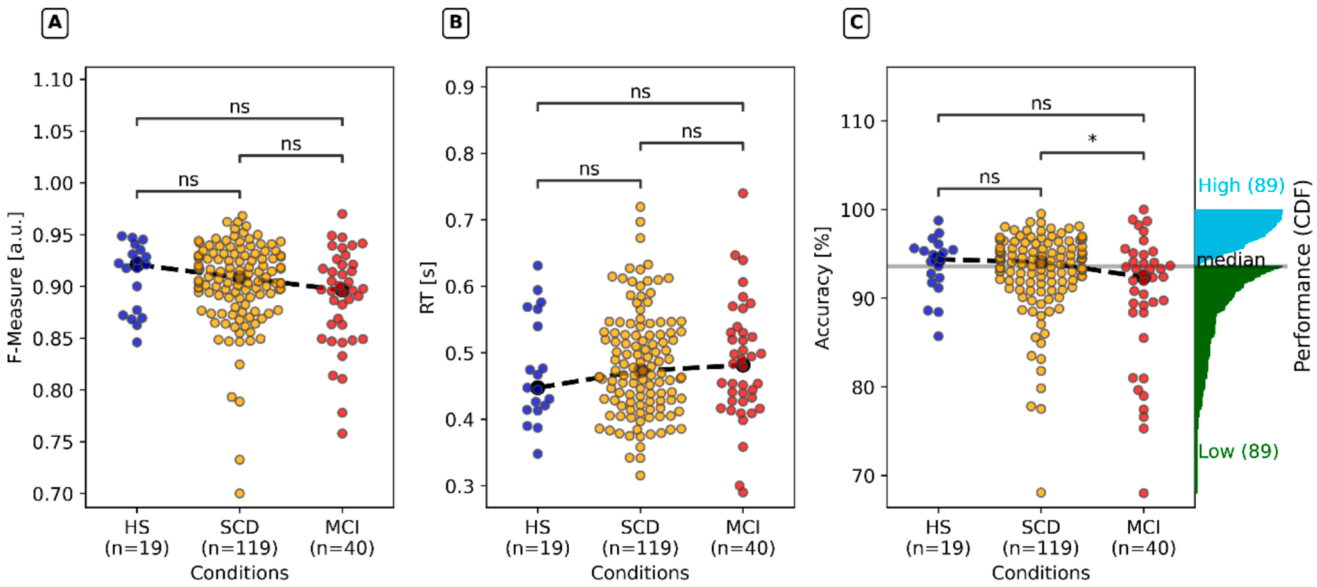

Fig. 2. Behavioural outcomes across conditions. (A) F-measure [a.u.]. (B) Reaction time [s]. (C) Accuracy [%]. To the right of (C) is the Cumulative Density Function of Accuracy dichotomised into 'low' and 'high' levels with reference to the median of the aggregated conditions. Pairwise statistics based on Kruskal-Wallis H test with p-value corrected by Bonferroni's method (alpha = 0.05). P-value annotation legend: ns: 0.05 < p <= 1, *: 0.01 < p <= 0.05, **: 0.001 < p <= 0.01, ***: 0.0001 < p <= 0.001. Colour code: HS (blue), SCD (orange), MCI (red), Low-performance subjects (green) and High-performance subjects (cyan). (For interpretation of the references to colour in this figure legend, the reader is referred to the web version of this article.)

significant deviations, although less pronounced than those observed in SCD. These findings suggest that while MCI subjects still exhibit relevant reductions compared to HS, the magnitude of change is more contained, consistent with a possible stabilization of some ERP metrics in the later stages. In the comparison between SCD and MCI (Fig. 5C), the differences were less evident. Significant deviations were found only in the P2 integral (−11.84 %), while the N1 integral (−15.82 %) showed smaller and non-significant variations. This result highlights that P2 represents the most sensitive integral in distinguishing SCD from MCI, capturing subtle differences between these two stages of cognitive decline. These analyses indicate that the integrals of N1 and P2 are the most consistent markers of cognitive decline, with significant deviations observed in both SCD and MCI compared to HS, and a greater sensitivity of P2 in differentiating between SCD and MCI.

3.5. SCD performance is modulated by distinct ERP dynamics in decision-making phases

After identifying electrophysiological correlates associated with the clinical conditions, we investigated the ERP correlates of task performance. In healthy subjects, significant differences were observed in the early time window (0–350 ms) within the N1 component (~80–120 ms), where the low-performance group exhibited a more pronounced negative deflection compared to the high-performance group (S-Fig. 3A). While no significant differences were detected in the P1 (~50 ms) or P2 (~150 ms) components, slight trends suggested potential performance-related variations. In the late time window (300–1000 ms), significant differences were identified in the P300 component (~350–450 ms), with the low-performance group showing a higher positive amplitude compared to the high-performance group (S-Fig. 3B). No significant differences were found for the P600 (~500–700 ms) or P900 (~800–1000 ms), though the low-performance group exhibited a tendency toward slightly higher amplitudes in these later components. These findings suggest that early attentional processing, as indicated by the N1 component (~80–120 ms), and late cognitive evaluation, as reflected in the P300 component (~350–450 ms), are key factors associated with differences in task performance among HS.

In SCD, ERP dynamics revealed significant differences between high and low performance groups during specific time windows. In the early phase (0–350 ms), significant differences were observed in the N1 component (~80–120 ms), where the low-performance group displayed a larger negative deflection compared to the high-performance group (Fig. 6 A). P1 (~50 ms) and P2 (~150 ms) did not show significant differences, though slight trends were evident. In the late phase (300–1000 ms), significant differences were found in the P300 component (~350–450 ms), with the high-performance group exhibiting a higher positive amplitude relative to the low-performance group (Fig. 6 B). No significant differences were detected for the P600 (~500–700 ms) or P900 (~800–1000 ms), though the high-performance group demonstrated a tendency for slightly higher amplitudes in these components. These results suggest that in SCD, early attentional processing, as reflected by the N1 component, and late cognitive evaluation, as indicated by the P300 component, are associated with differences in task performance. The absence of significant changes in later components such as P600 and P900 may indicate that these features are less sensitive to performance differences in SCD participants.

In MCI, ERP dynamics revealed no significant differences between high and low performance groups across early or late components. In the early time window (0–350 ms), components such as P1 (~50 ms), N1 (~80–120 ms), and P2 (~150 ms) showed similar waveforms across groups, with no statistically significant differences detected (Fig. 7A). Although slight trends were visible in the N1 component, these did not reach significance. In the late time window (300–1000 ms), components P300 (~350–450 ms), P600 (~500–700 ms), and P900 (~800–1000 ms) similarly exhibited no significant differences between the two groups (Fig. 7B). Both high and low performance groups demonstrated comparable ERP amplitudes, with overlapping confidence intervals throughout these later time periods. These findings suggest that in MCI, ERP dynamics across both early attentional processing and late cognitive evaluation components are less sensitive to performance differences. This may reflect a generalized reduction in neural reactivity or compensatory mechanisms that diminish group-level distinctions in task performance.

Features extraction of ERP in clinical conditions in relation to performance reveals distinct patterns between SCD and MCI (statistics reported in Table 3 for SCD and Table 4 for MCI). The analysis of ERP

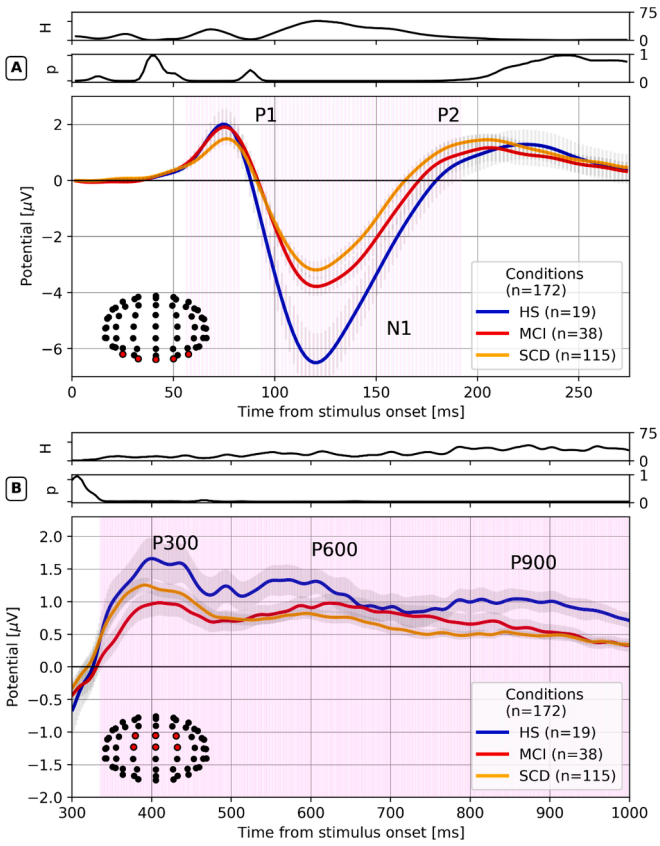

Fig. 3. ERP dynamics across conditions. (A). ERP computed as average of signals in the cluster of occipital channels (PO7, PO8, O1, Oz, O2) representative of the encoding phase of the stimulus. (B) ERP computed as average of signals in the cluster of central channels (FC1, FCz, FC2, C1, Cz, C2) representative of the decision-making phase regarding the stimulus. Both panels (A) and (B): Bold representation is the overall mean within each group and shading is the standard deviation. The measures on top are the instantaneous H-statistic of the Kruskal-Wallis test and the associated p-value corrected by Bonferroni's method (alpha < 0.05). Temporal instants associated with a $p < 0.05$ are highlighted with a vertical violet bar. P1/N1/P2 and P300/600/900 labels stand for the name of the event-related potentials relative to the encoding phase and decision-making phase, respectively. Colour code: HS (blue), SCD (orange), MCI (red). (For interpretation of the references to colour in this figure legend, the reader is referred to the web version of this article.)

features in SCD showed significant differences in latency and peak amplitude between Low and High performance groups, while the integral measures showed no substantial differences. High performers had significantly shorter latencies for the P1 component (63.66 ms vs. 69.29 ms, $p = 0.001$) and the N1 component (93.17 ms vs. 102.45 ms, $p = 0.004$), reflecting faster early sensory processing and attention allocation. Significant differences in peak amplitude were observed for the P300 (3.49 μV vs. 3.16 μV, $p = 0.0011$) and P600 (1.52 μV vs. 1.27 μV, $p = 0.0061$) components, suggesting enhanced cognitive processing and memory integration in High performers. The integral measures did not differ significantly, indicating that the total neural response energy remains stable across groups. These findings highlight performance-related differences in both early sensory (P1, N1) and later cognitive (P300, P600) processing stages in SCD. In contrast, the analysis of MCI revealed no statistically significant differences in ERP latency, peak amplitude, or integral across all components (as shown in Fig. 7). For latency, the P1 component was slightly shorter in the High group (64.38 ms vs. 66.45 ms, $p = 0.1184$), but the difference was not significant. Similarly, no significant differences were observed for the P2, N1, P300, P600, or P900 components. Peak amplitude and integral measures also showed no significant group differences. For instance, the P300 peak amplitude (2.99 μV vs. 3.09 μV, $p = 0.5956$) and the P1 integral (124.23 μV·ms vs. 139.96 μV·ms, $p = 0.0859$) were comparable across groups. In conclusion, SCD demonstrated clear performance-related differences in ERP features, whereas MCI exhibited more homogenous patterns.

3.6. ATN classification is associated with a specific ERP dynamic in SCD and MCI patients

After studying the ERP dynamics between clinical conditions and performance levels, we investigated the correlates of ATN classification. Our results showed that, aggregating SCD and MCI patients undergoing CSF examination ($N = 58$), no significant differences were observed between positive and negative ATN status along the temporal dynamics of encoding in occipital channels and decision-making in central channels (S-Fig. 4). However, when stratifying the ATN classification according to clinical condition, significant results emerged for both patients with SCD ($N = 34$) and MCI ($N = 24$). In SCDs (S-Fig. 5) a significant time window was found corresponding to N1 (Wang et al., 2024; Fabbrizzi et al., 2025; Sperling et al., 2011; Koenig et al., 2002; Lassi et al., 2023; Mielke, 2018; Mazure and Swendsen, 2016; Sundermann et al., 2019; Doan et al., 2021; Zhang et al., 2023; Kim et al., 2021; Rutkowski et al., 2023; Chedid et al., 2022; Ieracitano et al., 2020; Jae et al., 2023; Sibilano et al., 2024; Sibilano et al., 2023; Young et al., 2018; Arenaza-Urquijo et al., 2024; Frisoni et al., 2024; Sabri et al., 2015; Buerger et al., 2006), which represented an anticipatory time offset in case of a positive ATN. Stratifying the ATN by MCI condition (see S-Fig. 6), no significant differences were observed within the encoding window. However, differences were noted during the decision phase, in the attenuation of the amplitude peaks of P600 (476–591 ms) and P900 (750–945 ms, and spots over > 986 ms) in the case of ATN positive MCI.

3.7. Encoding FC reflects the non-monotonic ordering of ERP features

The analysis of encoding FC (%) reveals differences across conditions (HS, SCD, and MCI) but not related to performance levels (Fig. 8 A). In SCD, no significant differences were observed between Low and High performance groups ($p = 1.000$). Similarly, within MCI, Low and High groups also showed no significant differences in encoding FC ($p = 1.000$). However, a significant difference was observed between SCD and MCI ($p = 0.039$), suggesting changes in encoding FC related to disease progression, while HS vs. SCD approached significance ($p = 0.059$). For the ATN profiles (Fig. 8 B), comparisons within SCD (Negative vs. Positive) and MCI (Negative vs. Positive) yielded no significant differences ($p = 1.000$), indicating encoding FC does not appear to differentiate these groups. Overall, while performance-related differences were not significant within groups, the transition from SCD to MCI showed a meaningful drop in encoding FC, potentially reflecting underlying neural compensation or degeneration.

4. Discussion

Electrophysiological markers offer a unique window into cognitive decline, capturing neural dynamics that behavioral and clinical assessments alone cannot fully reveal. Unlike standard neuropsychological measures, ERPs provide real-time insights into sensory and cognitive processing, offering potential biomarkers for early classification and disease progression tracking. This study investigated clinical, behavioral, and neural measures in a cohort of 178 individuals (119 SCD, 40 MCI, 19 HS) during a sustained attention task to examine cognitive decline. MCI patients exhibited lower MMSE scores, and fewer years of education compared to SCD and HS, reinforcing the association between cognitive decline and clinical impairment. Accuracy was significantly lower in MCI patients compared to HS and SCD, while reaction time remained comparable across groups, suggesting that accuracy may serve as a more sensitive indicator of cognitive impairment than processing

Table 2
ERP features (latency, peak, integral) extracted from ERP dynamics across group conditions.

Type	ERP	SCD (N = 115)	MCI (N = 38)	HS (N = 19)	SCD vs MCI p(H)	SCD vs HS p(H)	MCI vs HS p(H)
Lat	P1	66.25 (22.04)	65.69 (15.01)	63.04 (16.79)	0.3535 (2.45)	0.099 (4.55)	1 (0.85)
Lat	P2	156.54 (30.04)	157.37 (30.62)	172.48 (30.75)	1 (0.21)	**** 0.0 (21.8)	*** 0.0003 (15.28)
Lat	N1	97.44 (37.53)	101.47 (26.68)	103.9 (17.32)	1 (0.74)	* 0.0239 (7.04)	0.2815 (2.81)
Lat	P300	351.34 (59.27)	356.34 (64.74)	362.26 (60.32)	0.5064 (1.89)	0.2675 (2.89)	1 (0.28)
Lat	P600	531.65 (96.4)	528.42 (93.78)	528.88 (92.01)	1 (0.12)	1 (0.04)	1 (0.0)
Lat	P900	934.81 (70.23)	917.93 (72.08)	927.79 (70.03)	** 0.004 (10.29)	0.8817 (1.1)	0.7358 (1.35)
Peak	P1	2.75 (2.31)	2.93 (1.75)	2.93 (2.23)	* 0.027 (6.82)	1 (0.74)	1 (0.79)
Peak	P2	5.87 (2.47)	6.14 (3.1)	5.43 (2.56)	1 (0.79)	0.4935 (1.93)	0.2674 (2.89)
Peak	N1	−0.25 (3.31)	−0.45 (2.51)	−3.46 (4.22)	0.164 (3.69)	**** 0.0 (50.78)	**** 0.0 (32.72)
Peak	P300	3.34 (1.56)	3.06 (1.57)	3.43 (1.66)	0.0839 (4.83)	1 (0.81)	0.0754 (5.01)
Peak	P600	1.4 (1.21)	1.58 (1.28)	1.8 (1.03)	* 0.0369 (6.27)	*** 0.0005 (14.37)	0.4182 (2.18)
Peak	P900	0.41 (1.03)	0.46 (1.01)	0.96 (1.1)	1 (0.57)	**** 0.0 (25.05)	*** 0.0005 (14.14)
Int	P1	132.7 (113.46)	134.16 (85.09)	162.18 (124.01)	0.5307 (1.82)	0.0863 (4.78)	0.5897 (1.67)
Int	P2	568.9 (337.54)	645.3 (322.53)	819.81 (420.93)	* 0.0136 (8.06)	**** 0.0 (33.18)	** 0.002 (11.55)
Int	N1	207.96 (213.91)	247.04 (198.54)	375.49 (246.17)	* 0.0358 (6.32)	**** 0.0 (37.1)	*** 0.0001 (16.83)
Int	P300	349.58 (196.78)	356.94 (189.35)	401.84 (197.36)	1 (0.55)	* 0.0164 (7.72)	0.1164 (4.27)
Int	P600	217.32 (185.72)	244.44 (183.75)	281.13 (183.48)	0.0877 (4.75)	*** 0.0008 (13.22)	0.2689 (2.88)
Int	P900	48.74 (143.62)	68.53 (144.07)	109.17 (153.84)	0.1293 (4.09)	*** 0.0001 (17.1)	0.06 (5.41)

Note. The table presents the mean and standard deviation (SD) for various Event-Related Potential (ERP) components measured in latency (Lat [ms]), peak amplitude (Peak [μV]), and integral amplitude (Int [μV × mS]) across three groups: Subjective Cognitive Decline (SCD, N = 115), Mild Cognitive Impairment (MCI, N = 38), and Healthy Subjects (HS, N = 19). Pairwise comparisons between groups (SCD vs. MCI, SCD vs. HS, MCI vs. HS) are shown with p-values (p(H)) from the Kruskal-Wallis test. Features correlations with age are indicated by p-values (p(r)) from the Spearman correlation test. Significant p-values are marked with asterisks: * ($p < 0.05$), ** ($p < 0.01$), *** ($p < 0.001$), **** ($p < 0.0001$).

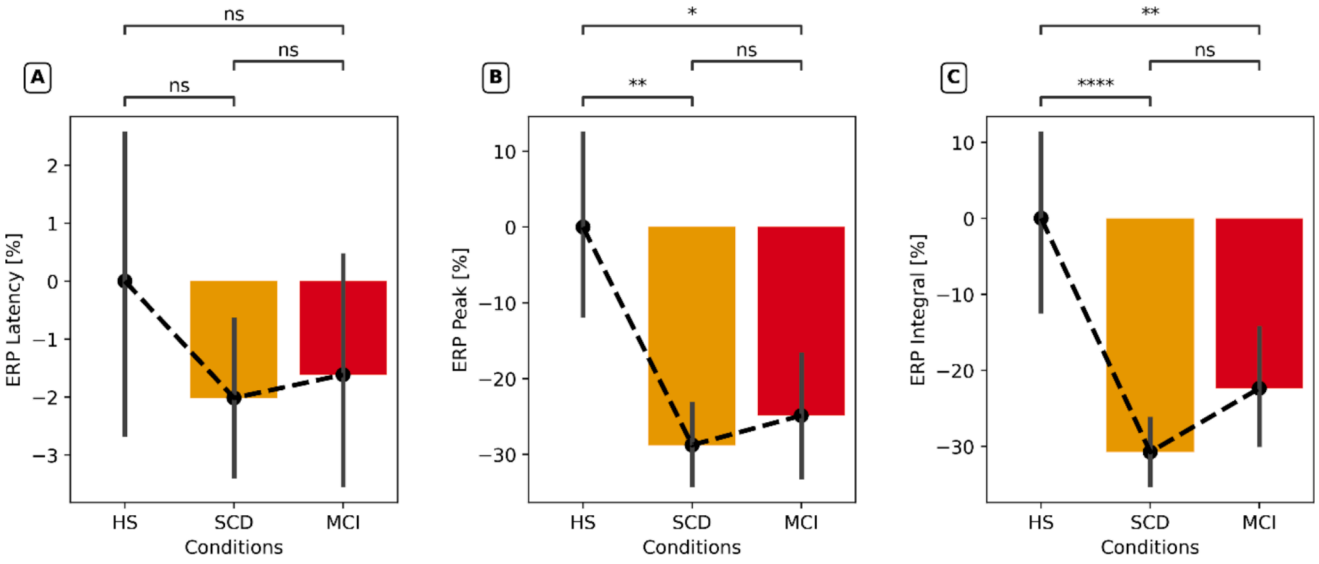

Fig. 4. Aggregated feature types normalized by HS values. The feature types (latency, peak, integral) aggregated the potentials (P1/N1/P2/P300/P600/P900) and are normalized by HS mean (0 % variations means the values are closed to HS average value; if % is > 0/<0 means positive/negative percentage deviation from HS mean). Each panel showed bar and line plots to highlight mono/non-monotonic trend. (A) ERP latency. (B) ERP peak. (C) ERP integral. Pairwise statistics based on Kruskal H test with p-value corrected by Bonferroni's method (alpha = 0.05). P-value annotation legend: ns: 0.05 < p <= 1, *: 0.01 < p <= 0.05, **: 0.001 < p <= 0.01, ***: 0.0001 < p <= 0.001. Colour code: SCD (orange), MCI (red). (For interpretation of the references to colour in this figure legend, the reader is referred to the web version of this article.)

speed. SCD patients, compared to HS, displayed attenuated sensory (P1, N1, P2) and cognitive (P300, P600, P900) components, although cognitive components exhibited performance-related gains. In contrast, MCI patients did not exhibit further attenuation but rather demonstrated compensatory enhancements, counteracting the decline observed in SCD. This non-monotonic pattern of ERP alterations suggests the engagement of adaptive neural mechanisms in MCI, potentially reflecting shifts in cognitive resource allocation.

4.1. *Visuo-attentive impairment along the cognitive decline*

These findings support the hypothesis that visual sensory abnormalities characterize SCD and MCI patients to varying degrees (Amariglio et al., 2012). For example, occipital P1 and N1 potentials are thought to represent aspects of visual-attentive processes, including their cost (P1) and benefit (N1) (Luck et al., 1990; Mangun and Hillyard, 1991; Clark et al., 1994). Open hypotheses suggest that P1 and N1 may not solely originate from the primary visual cortex, with N1 potentially linked to occipital-parietal/temporal/frontal generators (Woldorff et al., 1997), whereas P1 from extra V1 regions (V2,V3, dorsal V4) (Di Russo et al., 2002; Di Russo and Spinelli, 1999). Therefore, the recorded abnormalities in early visual components between SCD and MCI may indicate a broader impairment of the early attentional mechanism in visual processing (Golob et al., 2002). Moreover, P2 is associated with attention allocation and feature detection. In AD, P2 has been observed with significantly longer latencies and smaller slow wave amplitudes

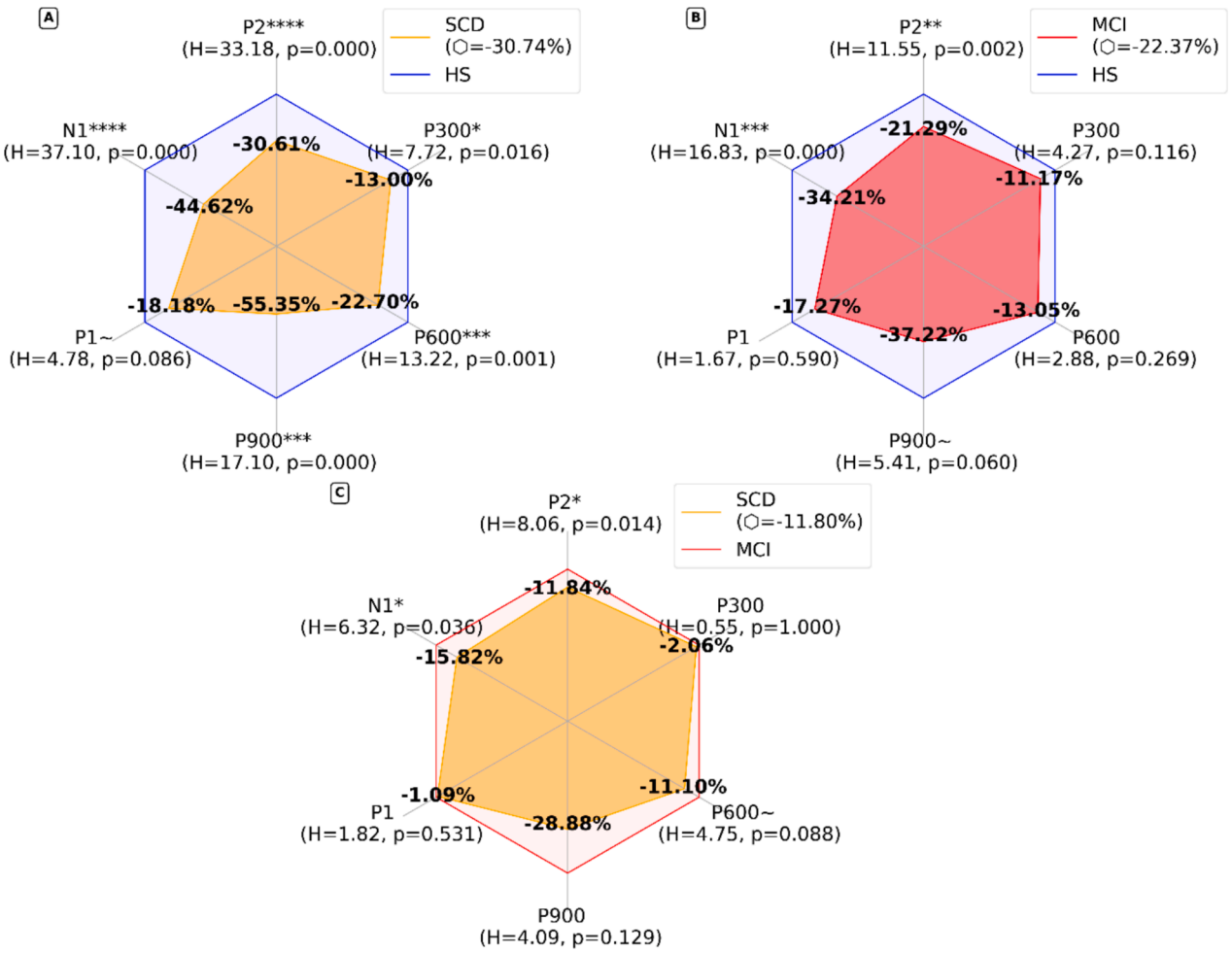

Fig. 5. Radar plots of normalized integral features. The graphs show the percentage deviations of each ERP integral feature from the HS case of the SCD (A) and MCI (B) conditions, and the percentage deviation of SCD from MCI (C). The hexagonal box on each radar plot represents the percentage limit of 0 % (HS for A-B and MCI for C), the positive or negative deviations of which show the variations from that reference. The numbers on the corner points of the polygon indicate the deviation in percentage terms for each integral characteristic. The legend shows the average of the percentage changes of the integrals (indicated by ⬡). The pairwise statistic based on the Kruskal H test with p-value corrected by Bonferroni's method (alpha = 0.05) is close to each percentage pair. Annotation legend P-value: ns: 0.01 < p <= 1, ~: 0.05 < p < 0.1, *: 0.01 < p <= 0.05, **: 0.001 < p <= 0.01, ***: 0.0001 < p <= 0.001. Colour code: HS (blue), SCD (orange), MCI (red). (For interpretation of the references to colour in this figure legend, the reader is referred to the web version of this article.)

(Golob et al., 2009; Oakley et al., 2025). A recent study (Gouvea et al., 2010), instead, found that P2 amplitudes significantly increased in MCI patients compared to non-MCI individuals, while the P300 amplitude was reduced, as expected. Additionally, the P2-to-P300 ratio was elevated in MCI patients, even in cases where P300 remained strong. This trend persisted in case studies tracking patients from early to later disease stages. These findings suggest that P2 alterations may serve as an early marker of MCI, especially in situations where P300 remains relatively preserved.

In our study, beyond sensorial components, we addressed cognitive ERPs as P300, P600 and P900, probed in central channels. P300 is a well-established ERP linked to the quality of decision making (Hedges et al., 2016; Polich et al., 1986; Braverman et al., 2006), while P600 e P900 are less explored components. The P600 is a late positive ERP that plays a key role in language comprehension and cognitive processing. Initially identified in response to syntactic anomalies, the P600 is often observed when readers or listeners encounter grammatical errors or com-plex sentence structures (Leckey and Federmeier, 2020). However, some researchers argue that it is not solely tied to syntactic reanalysis but may reflect broader re-evaluative and integrative cognitive processes (Sassenhagen et al., 2014). The P600-as-P3 hypothesis (Xia et al., 2024) suggests that this component shares characteristics with the P3b, indicating its role in attentional reallocation when unexpected linguistic inputs are encountered. Moreover, research has linked P600 abnormalities to neurodegenerative conditions and, in particular with MCI or preclinical AD found that P600 responses is altered (Olichney et al., 2008; Olichney et al., 2013), indicating its potential as an early biomarker for dementia risk. The P900 is a later ERP component that has been observed in various cognitive tasks. It is linked to semantic processing and neural compensation mechanisms, particularly in memory-related tasks in early AD (Rosenfeld and Labkovsky, 2010). Additionally, studies have identified P900 as a marker of countermeasure use in deception detection paradigms such as the P300-based Concealed Information Test (CIT) (Meixner et al., 2013; Hull and Harsh, 2001) and sleep-related cognitive states (Anderer et al., 2003).

Patients demonstrated cognitive decline in task performance, with the analysis of the P300 and P600 components revealing differences across clinical groups. In SCD, individuals with High performance showed enhanced P300 and P600 amplitudes compared to the Low performance group, indicating greater cognitive activation during decision-making and information integration. However, even in the Low performance group, these components were attenuated compared to HS controls, suggesting alterations in early cognitive processing mechanisms. In MCI, both P300 and P600 amplitudes were generally

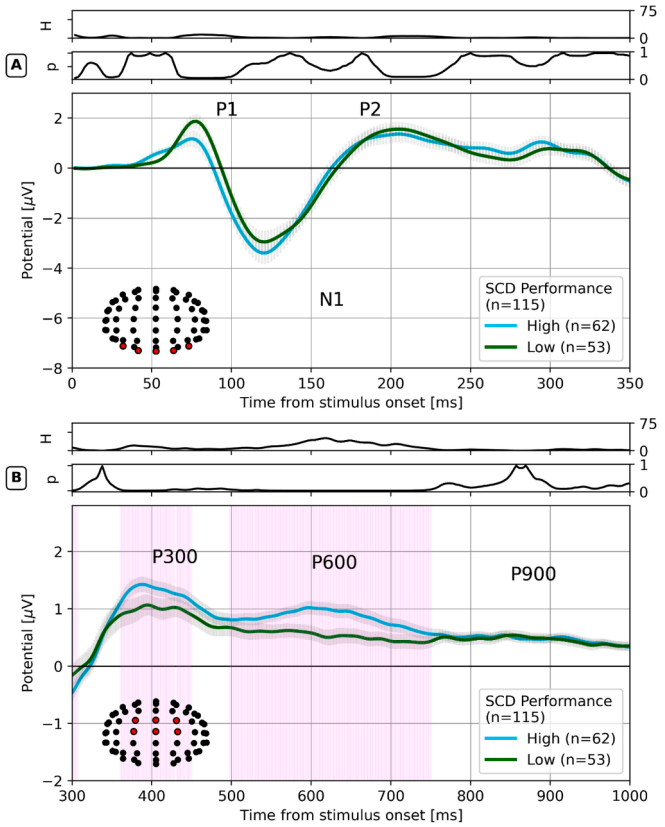

Fig. 6. ERP dynamics across performance in SCD. (A). ERP computed in the cluster of occipital channels (PO7, PO8, O1, Oz, O2) representative of the encoding phase of the stimulus. (B) ERP computed in cluster of central channels (FC1, FCz, FC2, C1, Cz, C2) representative of the decision-making phase regarding the stimulus. Both panels (A) and (B): Bold representation is the overall mean within each group and shading is the standard deviation. The measures on top are the instantaneous H-statistic of the Kruskal-Wallis test and the associated p-value corrected by Bonferroni's method (alpha < 0.05). Temporal instants associated with a $p < 0.05$ are highlighted with a vertical violet bar. P1/N1/P2 and P300/600/900 labels stand for the name of the event-related potentials relative to the encoding phase and decision-making phase respectively. Colour code: low performance subjects (green), high performance subjects (cyan). (For interpretation of the references to colour in this figure legend, the reader is referred to the web version of this article.)

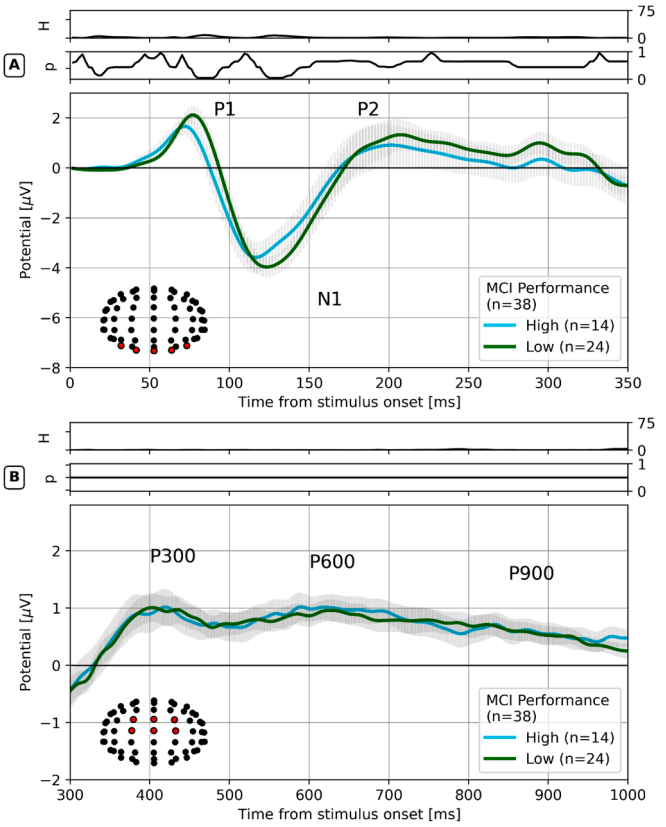

Fig. 7. ERP dynamics across performance in MCI. (A). ERP computed in the cluster of occipital channels (PO7, PO8, O1, Oz, O2) representative of the encoding phase of the stimulus. (B) ERP computed in cluster of central channels (FC1, FCz, FC2, C1, Cz, C2) representative of the decision-making phase regarding the stimulus. Both panels (A) and (B): Bold representation is the overall mean within each group and shading is the standard deviation. The measures on top are the instantaneous H-statistic of the Kruskal-Wallis test and the associated p-value corrected by Bonferroni's method (alpha < 0.05). Temporal instants associated with a $p < 0.05$ are highlighted with a vertical violet bar. P1/N1/P2 and P300/600/900 labels stand for the name of the event-related potentials relative to the encoding phase and decision-making phase respectively. Colour code: low performance subjects (green), high performance subjects (cyan). (For interpretation of the references to colour in this figure legend, the reader is referred to the web version of this article.)

attenuated compared to HS controls, but there was a greater amplification of P600 compared to SCD individuals, indicating potential compensatory mechanisms in response to cognitive deficits. No significant differences were observed between the High and Low performance groups within the MCI group, suggesting that disease progression may have a more uniform impact on information processing at this stage. Overall, the analysis of P300 and P600 reveals that in SCD, enhanced cognitive processing is associated with better performance, while in MCI, there is a more generalized attenuation, with some partial compensation in the P600 component. The relationship between P300 and P600 suggests that information processing is more compromised in MCI, though there are still signs of preserved cognitive activity in certain individuals. In fact, similar dynamics, but in the case of late positive potential (LPP) was found by Waninger et al which detected performance correlations with LPP recorded on parietal channels, but during a working load visual memory test that is the Standardized Image Recognition test (SIR) (Chapman and Bragdon, 1964). In general, across patients, P300, P600 and P900 were observed in our study to be attenuated in gain or latencies in the case of patients compared to HS. This results are in line with previous observations of P300 dynamics in relation to cognitive decline (Hedges et al., 2016; Polich et al., 1986; Braverman et al., 2006), or, regarding P600, which has been observed that its abnormalities are associated with increased risk of conversion to dementia in MCI patients (Olichney et al., 2008; Olichney et al., 2013; Dröge et al., 2016).

The reduction in P300 amplitudes associated with cognitive decline has been topographically linked to sources mainly in the medial frontal cortex, right dorsolateral prefrontal cortex, right inferior parietal lobe (Mulert et al., 2004), and in general in a non-pathological condition at the temporo-parietal junction (TPJ), supplementary motor cortex (SMA), anterior cingulate cortex (ACC), superior temporal gyrus (STG), insula, and dorsolateral prefrontal cortex (Theofilas et al., 2017). Since these anatomically highly interconnected brain regions are part of a network associated with sustained attention, explain why P300 gain is reduced in the case of the most severe cognitive pathology. Interestingly, the P300 is the only component that appears to show monotony with the clinical condition, i.e. its attenuation follows the severity of the clinical condition. On the other hand, modulation of P600 appears to be associated with cognitive alterations of a linguistic nature (Leckey and Federmeier, 2020; Sassenhagen et al., 2014), and the generating sources may also involve the basal ganglia (Quinzi et al., 2020; Speer and Soldan, 2015). Although most studies on P600 are linguistic, it appears to

Table 3
ERP features (latency, peak, integral) extracted from ERP dynamics across task performance in SCD.

Type	ERP	Low (N = 53)	High (N = 62)	Low vs High p(H)
Lat	P1	69.29 (19.81)	63.66 (23.47)	*** 0.001 (10.86)
Lat	P2	157.79 (27.26)	155.47 (32.2)	0.307 (1.04)
Lat	N1	102.45 (41.84)	93.17 (32.8)	** 0.004 (8.29)
Lat	P300	352.76 (61.07)	350.12 (57.66)	0.5142 (0.43)
Lat	P600	532.72 (99.24)	530.74 (93.89)	0.9603 (0.0)
Lat	P900	939.07 (68.12)	931.17 (71.78)	0.1223 (2.39)
Peak	P1	2.77 (2.24)	2.72 (2.37)	0.7143 (0.13)
Peak	P2	5.67 (2.42)	6.04 (2.5)	0.1635 (1.94)
Peak	N1	−0.01 (3.0)	−0.46 (3.53)	0.2877 (1.13)
Peak	P300	3.16 (1.72)	3.49 (1.39)	** 0.0011 (10.63)
Peak	P600	1.27 (1.23)	1.52 (1.18)	** 0.0061 (7.53)
Peak	P900	0.41 (1.0)	0.41 (1.05)	0.5175 (0.42)
Int	P1	129.24 (104.58)	135.65 (120.46)	0.7791 (0.08)
Int	P2	564.6 (320.49)	572.58 (351.42)	0.9342 (0.01)
Int	N1	206.09 (208.13)	209.55 (218.71)	0.8807 (0.02)
Int	P300	343.06 (210.29)	355.15 (184.26)	0.1227 (2.38)
Int	P600	203.63 (169.7)	229.01 (197.65)	0.0929 (2.82)
Int	P900	46.98 (141.08)	50.25 (145.74)	0.452 (0.57)

Note. The table presents the mean and standard deviation (SD) for various Event-Related Potential (ERP) components measured in latency (Lat [ms]), peak amplitude (Peak [μV]), and integral amplitude (Int [μV × mS]) across two SCD groups: low performance (N = 59) and high performance (N = 55). Pairwise comparisons between groups are shown with p-values (p(H)) from the Kruskal-Wallis test. Features correlations with age are indicated by p-values (p(r)) from the Spearman correlation test. Significant p-values are marked with asterisks: * ($p < 0.05$), ** ($p < 0.01$), *** ($p < 0.001$), **** ($p < 0.0001$).

Table 4
ERP features (latency, peak, integral) extracted from ERP dynamics across task performance in MCI.

Type	ERP	High (N = 14)	Low (N = 24)	High vs Low p(H)
Lat	P1	64.38 (15.16)	66.45 (14.86)	0.1184 (2.44)
Lat	P2	155.65 (30.13)	158.36 (30.86)	0.5938 (0.28)
Lat	N1	104.71 (32.44)	99.57 (22.43)	0.5611 (0.34)
Lat	P300	358.44 (65.42)	355.11 (64.31)	0.84 (0.04)
Lat	P600	538.97 (84.96)	522.26 (98.03)	0.1308 (2.28)
Lat	P900	920.43 (76.02)	916.48 (69.64)	0.9917 (0.0)
Peak	P1	2.82 (1.6)	2.99 (1.82)	0.6957 (0.15)
Peak	P2	5.52 (2.65)	6.51 (3.28)	0.1741 (1.85)
Peak	N1	−0.45 (2.81)	−0.45 (2.31)	0.8098 (0.06)
Peak	P300	2.99 (1.54)	3.09 (1.59)	0.5956 (0.28)
Peak	P600	1.57 (1.02)	1.59 (1.42)	0.7835 (0.08)
Peak	P900	0.44 (1.02)	0.46 (1.0)	0.5365 (0.38)
Int	P1	124.23 (86.28)	139.96 (83.84)	0.0859 (2.95)
Int	P2	653.3 (304.6)	640.64 (332.46)	0.6577 (0.2)
Int	N1	245.97 (191.78)	247.67 (202.38)	0.8848 (0.02)
Int	P300	354.87 (175.34)	358.15 (197.05)	0.9419 (0.01)
Int	P600	222.72 (172.64)	257.11 (188.78)	0.1842 (1.76)
Int	P900	57.79 (137.33)	74.8 (147.51)	0.4028 (0.7)

Note. The table presents the mean and standard deviation (SD) for various Event-Related Potential (ERP) components measured in latency (Lat [ms]), peak amplitude (Peak [μV]), and integral amplitude (Int [μV × mS]) across two MCI groups: low performance (N = 26) and high performance (N = 12). Pairwise comparisons between groups are shown with p-values (p(H)) from the Kruskal-Wallis test. Features correlations with age are indicated by p-values (p(r)) from the Spearman correlation test. Significant p-values are marked with asterisks: * ($p < 0.05$), ** ($p < 0.01$), *** ($p < 0.001$), **** ($p < 0.0001$).

be related to the systemic release of norepinephrine by the locus coeruleus (Xia et al., 2024), which influences the quality of decision making, memory, and attention (Tomlinson et al., 1981), the cells of which are known to be profoundly reduced in the case of AD (Tomlinson et al., 1981; Mather and Harley, 2016; Matchett et al., 2021; Bartus et al., 1982; Betts et al., 2019; Cabeza et al., 2002).

4.2. Cognitive reserve, encoding FC and non-monotonic ERP trend

Cognitive reserve (CR) is recognized for its role in influencing cognitive decline, potentially shielding against dementia symptoms despite existing brain alterations (Stern, 2006). SCD patients exhibited higher proxy scores of CR compared to MCI patients, as evidenced by measures of leisure activities and clinical scales. This suggests a potentially greater capacity for brain resilience in supporting cognitive functions among SCD patients. The CR is related to the concept of brain efficiency (Stern et al., 2003; Cabeza et al., 2018; Gu et al., 2018), i.e., lower utilization of cortical activity for getting performance, in fact its contrary – neural inefficiency – has been associated with low CR (Habeck et al., 2003; Gajewski et al., 2020). The overuse of neural resources during the performance of a task is known to increase in relation to age, particularly the extra-engagement of prefrontal cortex, and modulated by factors influencing CR such as IQ (Berchicci et al., 2012) and sport practice (Berchicci et al., 2013; Ramchandran et al., 2019).

In our study, we observed that MCI patients exhibited higher Encoding FC compared to SCD patients, suggesting a higher utilization of cognitive resources to perform the task. Additionally, the non-monotonicity of the observed features aligns with the general amplification of scalp activity in MCI patients compared to SCD patients, which may also reflect deficits in brain efficiency. Our results are in line with studies showing brain efficiency in terms of adaptive control of neural resource consumption (Lipp et al., 2012; Fischer et al., 2021), in particular in AD and related conditions (Stern et al., 2023; Mevel et al., 2011; Fischer et al., 2023).

Hence, the non-monotonic ordering of features could be explained by the brain inefficiency that some patients have, particularly MCI patients who showed the greatest extra-occipital recruitment. In this sense, modelling neural inefficiency could add causal contributions with respect to cognitive reserve and the underlying biophysical factors (Lavanga et al., 2023). A cause-effect paradigm as a modelling framework (Amato et al., 2024; Monteverdi et al., 2022; Monteverdi et al., 2023; Wang et al., 2024; Fabbrizzi et al., 2025; Sperling et al., 2011) of pathological AD-type neural degeneration could explain the mechanisms underlying the observed non-monotonicity in scalp potentials, and thus explaining why the electrophysiological correlate does not follow a monotonic change in line with the continuous gradient of cognitive decline (Fig. 1 in (Koenig et al., 2002).

Of note, SCD patients, showing less scalp similarity with the occipital seed compared to other channels, reflected a reduced dipole effect on the scalp, whereas HS and MCIs exhibited a dipole topography characterized by occipital negativity and frontal positivity when using higher neural resources. This occipito-frontal dipole pattern alterations resembles EEG microstate classes C and D (Lassi et al., 2023), which have been associated with AD and non-AD conditions in recent research (Mielke, 2018).

4.3. Strengths and weakness

Strengths include large sample size, multimodal data (EEG and patient descriptors), and inclusion of CSF markers in a subset. Weaknesses: limited robustness of CSF markers' statistical significance, low healthy subject number (focused on SCD vs. MCI), monocentric study without follow-ups (ongoing in PREVIEW study). Biological sex was not included as a factor modulating the results in this analysis. However, the sample reflects the typical sex distribution observed in dementia onset. Specifically, in our cohort of 178 individuals, 65.73 % were female and 34.27 % were male. Among the 119 patients with SCD, 71.43 % were female and 28.57 % were male; among the 40 MCI patients, 60.0 % were female and 40.0 % were male. These proportions are consistent with epidemiological data indicating a higher prevalence of dementia in women. Studies have shown that women account for approximately two-thirds of Alzheimer's disease cases (Mazure and Swendsen, 2016; Sundermann et al., 2019), likely due to a combination of biological, genetic, and

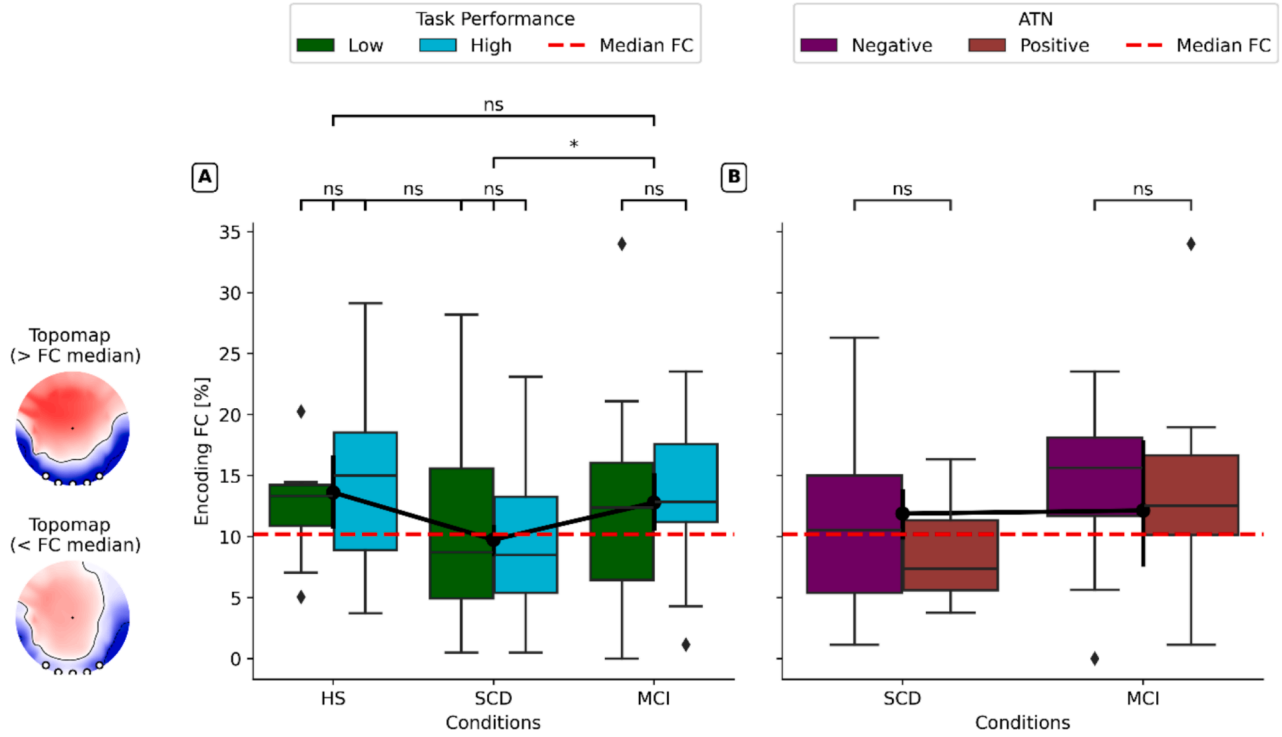

Fig. 8. Encoding FC computed across clinical conditions and ATN classification. (A) Boxplot of clinical conditions. (B) Boxplot of clinical conditions stratified by ATN status. Topographic maps left to (A) are indicative of the scalp potentials spread during the encoding process (0–200 ms) as the FC is over/under the FC median. Colormaps are in voltage range −1/+1 [μV]. Higher FC means higher similarity between the occipital seed and other channels, indicative of increased extra-occipital scalp recruitment. Pairwise comparisons between groups are shown with p-values from the Kruskal-Wallis test. Significant p-values are marked with asterisks: * ($p < 0.05$), ** ($p < 0.01$), *** ($p < 0.001$), **** ($p < 0.0001$).

lifestyle factors, including longevity and hormonal influences. Furthermore, research suggests that the female-to-male ratio is particularly high in early stages such as SCD and MCI, reflecting the general pattern of higher lifetime risk for women (Doan et al., 2021).

4.4. *Future works*

A direct application of the ERP neural features identified in this study is training machine learning algorithms to classify patients based on learned diagnostic categories (Rossini et al., 2022; Zhang et al., 2023; Kim et al., 2021; Rutkowski et al., 2023; Chedid et al., 2022; Ieracitano et al., 2020; Jae et al., 2023; Sibilano et al., 2024; Sibilano et al., 2023; Young et al., 2018; Arenaza-Urquijo et al., 2024). It is important to consider the potential role of misclassifications, particularly the assignment of a clinical category that may not accurately reflect the severity of the condition. For example, misclassifying an SCD patient as MCI may imply a neural correlation more aligned with greater neurophysiological and biological alterations, potentially signifying a higher risk for cognitive decline. Therefore, when applying machine learning to features extracted from neural correlates, it is essential to assess not only the algorithm's technical error (i.e., false misclassifications) but also the potential clinical implications of these misclassifications, as they could provide valuable insights into the patient's clinical trajectory. Moreover, given the increasing recognition of sex as a critical factor in neurodegeneration (Frisoni et al., 2024), future studies will explicitly address its influence on cognitive trajectories and disease progression.

5. Conclusion

Current cognitive decline biomarkers (Sabri et al., 2015), such as PET neuroimaging (Buerger et al., 2006) or CSF biomarkers (Mengel et al., 2024), are costly, invasive, and impractical for large-scale use. Our study aims to overcome these limitations by exploring features obtainable through clinical assessments, neuropsychological evaluations, and non-invasive methods like EEG and blood tests (Babiloni et al., 2020). ERP dynamics, in particular, revealed critical discontinuities in cognitive decline, challenging the assumption of a linear progression from health to pathology. These deviations could reflect compensatory mechanisms and cerebral resilience, disrupting expected ERP monotonicity. Our methodology captures these nonlinear changes, offering insights beyond standard markers like amplitude attenuation or latency slowing, which fail to account for the brain's adaptive strategies and underlying neurobiological alterations. Validating multiple EEG/ERP neural features (Sabri et al., 2015; Horvath et al., 2018; Knopman, 2024) is crucial to establish their preventive and diagnostic potential for Alzheimer's disease and, in general, along the cognitive decline continuum, in order to improve and support the clinical decision-making (Mazzeo et al., 2024).

Funding sources

This project was funded by Tuscany Region – PRedicting the EVolution of SubjectIvE Cognitive Decline to Alzheimer's Disease With machine learning – PREVIEW – CUP. D18D20001300002 and by Project funded under the National Recovery and Resilience Plan (NRRP), Mission 4 Component 2 Investment 1.3 – Call for tender No. 341 of 15/03/2022 of Italian Ministry of University and Research - funded by the European Union – NextGenerationEU Award Number: Project code PE0000006, Concession Decree No. 1553 of 11/10/2022 adopted by the Italian Ministry of University and Research, CUP D93C22000930002, "A multiscale integrated approach to the study of the nervous system in healt and disease" (MNESYS).

CRediT authorship contribution statement

A.A. Vergani: Writing – review & editing, Writing – original draft,

Visualization, Software, Formal analysis, Data curation, Conceptualization. **S. Mazzeo:** Writing – review & editing, Writing – original draft, Methodology, Formal analysis, Data curation, Conceptualization. **V. Moschini:** Writing – review & editing, Writing – original draft, Methodology, Formal analysis, Data curation, Conceptualization. **R. Burali:** Writing – review & editing, Methodology, Investigation, Conceptualization. **M. Lassi:** Writing – review & editing, Writing – original draft, Software, Methodology, Formal analysis, Data curation, Conceptualization. **L.G. Amato:** Writing – review & editing, Writing – original draft, Methodology, Formal analysis, Data curation, Conceptualization. **J. Carpaneto:** Writing – review & editing, Writing – original draft, Project administration, Methodology, Formal analysis, Data curation, Conceptualization. **G. Salvestrini:** Writing – review & editing, Writing – original draft, Methodology, Data curation, Conceptualization. **C. Fabbiani:** Writing – review & editing, Writing – original draft, Methodology, Data curation, Conceptualization. **G. Giacomucci:** Writing – review & editing, Writing – original draft, Methodology, Data curation, Conceptualization. **C. Morinelli:** Writing – review & editing, Writing – original draft, Methodology, Data curation, Conceptualization. **F. Emiliani:** Writing – review & editing, Writing – original draft, Methodology, Data curation, Conceptualization. **M. Scarpino:** Writing – review & editing, Writing – original draft, Methodology, Data curation, Conceptualization. **S. Bagnoli:** Writing – review & editing, Writing – original draft, Methodology, Data curation, Conceptualization. **A. Ingannato:** Writing – review & editing, Writing – original draft, Methodology, Data curation, Conceptualization. **B. Nacmias:** Writing – review & editing, Supervision, Methodology, Investigation, Conceptualization. **S. Padiglioni:** Writing – review & editing, Writing – original draft, Project administration, Methodology, Data curation, Conceptualization. **S. Sorbi:** Writing – review & editing, Supervision, Funding acquisition, Conceptualization. **V. Bessi:** Writing – review & editing, Writing – original draft, Supervision, Methodology, Investigation, Funding acquisition, Data curation, Conceptualization. **A. Grippo:** Writing – review & editing, Writing – original draft, Supervision, Methodology, Investigation, Data curation, Conceptualization. **A. Mazzoni:** Writing – review & editing, Writing – original draft, Supervision, Methodology, Investigation, Conceptualization.

Declaration of competing interest

The authors declare that they have no known competing financial interests or personal relationships that could have appeared to influence the work reported in this paper.

Acknowledgements

We thank Ahmet Kaymak, Nicolò Meneghetti, Fabio Taddeini, Giovanni Vecchiato, Giacomo Privato, Salvatore Falciglia, Michelangelo Fabbrizzi, Michela Rocchetti and Greta Carnevali for their relevant comments which have improved the quality of the research work. We also thank the reviewers for their comments which have improved the quality of the results.

Appendix A. Supplementary data

Supplementary data to this article can be found online at https://doi.org/10.1016/j.nicl.2025.103760.

Data availability

Data will be made available on request.

References

Albert, M.S., DeKosky, S.T., Dickson, D., Dubois, B., Feldman, H.H., Fox, N.C., et al., 2011. The diagnosis of mild cognitive impairment due to Alzheimer's disease: recommendations from the National Institute on Aging-Alzheimer's Association workgroups on diagnostic guidelines for Alzheimer's disease. Alzheimers Dement. 7 (3), 270–279.

Alcolea, D., Pegueroles, J., Muñoz, L., Camacho, V., López-Mora, D., Fernández-León, A., et al., 2019. Agreement of amyloid PET and CSF biomarkers for Alzheimer's disease on Lumipulse. Ann. Clin. Transl. Neurol. 6 (9), 1815–1824.

Alexander, D.M., Arns, M.W., Paul, R.H., Rowe, D.L., Cooper, N., Esser, A.H., et al., 2006. Eeg markers for cognitive decline in elderly subjects with subjective memory complaints. J. Integr. Neurosci. 05 (01), 49–74.

Amariglio, R.E., Becker, J.A., Carmasin, J., Wadsworth, L.P., Lorius, N., Sullivan, C., et al., 2012. Subjective cognitive complaints and amyloid burden in cognitively normal older individuals. Neuropsychologia 50 (12), 2880–2886.

Amato, L.G., Vergani, A.A., Lassi, M., Fabbiani, C., Mazzeo, S., Burali, R., et al., 2024. Personalized modeling of Alzheimer's disease progression estimates neurodegeneration severity from EEG recordings. Alzheimer's & Dementia: Diagnosis, Assessment & Disease Monit. 16 (1), e12526.

Anderer, P., Saletu, B., Semlitsch, H.V., Pascual-Marqui, R.D., 2003. Non-invasive localization of P300 sources in normal aging and age-associated memory impairment. Neurobiol. Aging 24 (3), 463–479.

Arenaza-Urquijo, E.M., Boyle, R., Casaletto, K., Anstey, K.J., Vila-Castelar, C., Colverson, A., et al., 2024. Sex and gender differences in cognitive resilience to aging and Alzheimer's disease. Alzheimer's & Dementia, n/a(n/a). Available from: https://onlinelibrary.wiley.com/doi/abs/10.1002/alz.13844.

Argiris, G., Stern, Y., Habeck, C., 2024. Brain Resilience to Targeted Attack of Resting BOLD Networks as a Measure of Cognitive Reserve. Res Sq., rs.3.rs-5356022.

Argiris, G., Stern, Y., Habeck, C., 2023. Neural similarity across task load relates to cognitive reserve and brain maintenance measures on the Letter Sternberg task: a longitudinal study. Brain Imaging Behav. 17 (1), 100–113.

Armstrong, R.A., 2009. Alzheimer's disease and the eye. J. Optometry 2 (3), 103–111.

Babiloni, C., Visser, P.J., Frisoni, G., De Deyn, P.P., Bresciani, L., Jelic, V., et al., 2010. Cortical sources of resting EEG rhythms in mild cognitive impairment and subjective memory complaint. Neurobiol. Aging 31 (10), 1787–1798.

Babiloni, C., Blinowska, K., Bonanni, L., Cichocki, A., De Haan, W., Del Percio, C., et al., 2020. What electrophysiology tells us about Alzheimer's disease: a window into the synchronization and connectivity of brain neurons. Neurobiol. Aging 1 (85), 58–73.

Balart-Sánchez, S.A., Bittencourt, M., van der Naalt, J., Maurits, N.M., 2024. Lower cognitive reserve is related to worse working memory performance in older adults after mTBI. An ERP Study. Brain Inj. 38 (7), 550–558.

Bartus, R.T., Dean, R.L., Beer, B., Lippa, A.S., 1982. The cholinergic hypothesis of geriatric memory dysfunction. Science 217 (4558), 408–414.

Barulli, D., Stern, Y., 2013. Efficiency, capacity, compensation, maintenance, plasticity: emerging concepts in cognitive reserve. Trends Cogn. Sci. 17 (10), 502–509.

Berchicci, M., Lucci, G., Pesce, C., Spinelli, D., Di Russo, F., 2012. Prefrontal hyperactivity in older people during motor planning. Neuroimage 62 (3), 1750–1760.

Berchicci, M., Lucci, G., Di Russo, F., 2013. Benefits of physical exercise on the aging brain: the role of the prefrontal cortex. J. Gerontol.: Series a. 68 (11), 1337–1341.

Betts, M.J., Cardenas-Blanco, A., Kanowski, M., Spottke, A., Teipel, S.J., Kilimann, I., et al., 2019. Locus coeruleus MRI contrast is reduced in Alzheimer's disease dementia and correlates with CSF Aβ levels. Alzheimer's & Dementia: Diagnosis, Assessment & Disease Monitoring. 1 (11), 281–285.

Braverman, E.R., Chen, T.J.H., Schoolfield, J., Martinez-Pons, M., Arcuri, V., Varshavskiy, M., et al., 2006. Delayed P300 latency correlates with abnormal Test of Variables of Attention (TOVA) in adults and predicts early cognitive decline in a clinical setting. Adv. Therapy 23 (4), 582–600.

Budd Haeberlein, S., Aisen, P.S., Barkhof, F., Chalkias, S., Chen, T., Cohen, S., et al., 2022. Two randomized phase 3 studies of aducanumab in early Alzheimer's disease. J. Prev. Alzheimers Dis. 9 (2), 197–210.

Buerger, K., Ewers, M., Pirttilä, T., Zinkowski, R., Alafuzoff, I., Teipel, S.J., et al., 2006. CSF phosphorylated tau protein correlates with neocortical neurofibrillary pathology in Alzheimer's disease. Brain 129 (Pt 11), 3035–3041.

Buss, S.S., Fried, P.J., Macone, J., Zeng, V., Zingg, E., Santarnecchi, E., et al., 2023. Greater cognitive reserve is related to lower cortical excitability in healthy cognitive aging, but not in early clinical Alzheimer's disease. Front. Hum. Neurosci. 17, 1193407.

Cabeza, R., Anderson, N., Locantore, J., Mcintosh, A., 2002. Aging gracefully: compensatory brain activity in high-performing older adults. Neuroimage 17 (3), 1394–1402.

Cabeza, R., Albert, M., Belleville, S., Craik, F.I.M., Duarte, A., Grady, C.L., et al., 2018. Maintenance, reserve and compensation: the cognitive neuroscience of healthy ageing. Nat. Rev. Neurosci. 19 (11), 701–710.

Chapman, R.M., Bragdon, H.R., 1964. Evoked responses to numerical and non-numerical visual stimuli while problem solving. Nature 203 (4950), 1155–1157.

Che, J., Cheng, N., Jiang, B., Liu, Y., Liu, H., Li, Y., et al., 2024. Executive function measures of participants with mild cognitive impairment: systematic review and meta-analysis of event-related potential studies. Int. J. Psychophysiol. 1 (197), 112295.

Chedid, N., Tabbal, J., Kabbara, A., Allouch, S., Hassan, M., 2022. The development of an automated machine learning pipeline for the detection of Alzheimer's Disease. Sci. Rep. 12 (1), 18137.

Cintra, M.T.G., Ávila, R.T., Soares, T.O., Cunha, L.C.M., Silveira, K.D., de Moraes, E.N., et al., 2018. Increased N200 and P300 latencies in cognitively impaired elderly carrying ApoE ε-4 allele. Int. J. Geriatr. Psychiatry 33 (2), e221–e227.

Clark, V.P., Fan, S., Hillyard, S.A., 1994. Identification of early visual evoked potential generators by retinotopic and topographic analyses. Hum. Brain Mapp. 2 (3), 170–187.

Danjou, P., Viardot, G., Maurice, D., Garcés, P., Wams, E.J., Phillips, K.G., et al., 2019. Electrophysiological assessment methodology of sensory processing dysfunction in schizophrenia and dementia of the Alzheimer type. Neurosci. Biobehav. Rev. 1 (97), 70–84.

Delorme, A., Makeig, S., 2004. EEGLAB: an open source toolbox for analysis of single-trial EEG dynamics including independent component analysis. J. Neurosci. Methods 134 (1), 9–21.

Devos, H., Gustafson, K.M., Liao, K., Ahmadnezhad, P., Kuhlmann, E., Estes, B.J., et al., 2023. Effect of cognitive reserve on physiological measures of cognitive workload in older adults with cognitive impairments. J. Alzheimers Dis. 92 (1), 141–151.

Di Russo, F., Martínez, A., Sereno, M.I., Pitzalis, S., Hillyard, S.A., 2002. Cortical sources of the early components of the visual evoked potential. Hum. Brain Mapp. 15 (2), 95–111.

Di Russo, F., Spinelli, D., 1999. Electrophysiological evidence for an early attentional mechanism in visual processing in humans. Vision Res. 39 (18), 2975–2985.

Doan, D.N.T., Ku, B., Choi, J., Oh, M., Kim, K., Cha, W., et al., 2021. Predicting dementia with prefrontal electroencephalography and event-related potential. Available from: Front. Aging Neurosci. 13 https://www.frontiersin.org/journals/aging-neuroscience/articles/10.3389/fnagi.2021.659817/full.

Dröge, A., Fleischer, J., Schlesewsky, M., Bornkessel-Schlesewsky, I., 2016. Neural mechanisms of sentence comprehension based on predictive processes and decision certainty: Electrophysiological evidence from non-canonical linearizations in a flexible word order language. Brain Res. 15 (1633), 149–166.

Dukart, J., Schroeter, M.L., Mueller, K., Initiative, T.A.D.N., 2011. Age correction in dementia – matching to a healthy brain. PLoS One 6 (7), e22193.

Fabbrizzi, M., Amato, L.G., Martinelli, L., Carpaneto, J., Bartolini, E., Calderoni, S., et al, 2025. Reconstructing whole-brain structure and dynamics using imaging data and personalized modeling [Internet]. medRxiv; p. 2025.01.06.24319726. Available from: https://www.medrxiv.org/content/10.1101/2025.01.06.24319726v1.

Fischer, F.U., Wolf, D., Tüscher, O., Fellgiebel, A., 2021. On behalf of Alzheimer's disease neuroimaging initiative. structural network efficiency predicts resilience to cognitive decline in elderly at risk for Alzheimer's Disease. Front. Aging Neurosci. 13. Available from: https://www.frontiersin.org/journals/aging-neuroscience/articles/10.3389/fnagi.2021.637002/full.

Fischer, F.U., Gerber, S., Tüscher, O., 2023. Initiative the ADN. A mathematical model of the Alzheimer's Disease biomarker cascade demonstrates statistical pitfalls in identifying neurobiological surrogates of cognitive reserve [Internet]. bioRxiv; p. 2023.10.26.563793. Available from: https://www.biorxiv.org/content/10.1101/2023.10.26.563793v1.

Frisoni, G.B., Festari, C., Massa, F., Ramusino, M.C., Orini, S., Aarsland, D., et al., 2024. European intersocietal recommendations for the biomarker-based diagnosis of neurocognitive disorders. Lancet Neurol. 23 (3), 302–312.

Gajewski, P.D., Falkenstein, M., Thönes, S., Wascher, E., 2020. Stroop task performance across the lifespan: High cognitive reserve in older age is associated with enhanced proactive and reactive interference control. Neuroimage 15 (207), 116430.

Ganapathi, A.S., Glatt, R.M., Bookheimer, T.H., Popa, E.S., Ingemanson, M.L., Richards, C.J., et al., 2022. Differentiation of subjective cognitive decline, mild cognitive impairment, and dementia using qEEG/ERP-based cognitive testing and volumetric MRI in an outpatient specialty memory clinic. J. Alzheimer's Dis. 90 (4), 1761–1769.

Gauthier, S., Reisberg, B., Zaudig, M., Petersen, R.C., Ritchie, K., Broich, K., et al., 2006. Mild cognitive impairment. Lancet 367 (9518), 1262–1270.

Giacomucci, G., Mazzeo, S., Bagnoli, S., Casini, M., Padiglioni, S., Polito, C., et al., 2021. Matching clinical diagnosis and amyloid biomarkers in Alzheimer's disease and frontotemporal dementia. J. Personalized Med. 11 (1), 47.

Golob, E.J., Johnson, J.K., Starr, A., 2002. Auditory event-related potentials during target detection are abnormal in mild cognitive impairment. Clin. Neurophysiol. 113 (1), 151–161.

Golob, E.J., Ringman, J.M., Irimajiri, R., Bright, S., Schaffer, B., Medina, L.D., et al., 2009. Cortical event-related potentials in preclinical familial Alzheimer disease. Neurology 73 (20), 1649–1655.

Gouvea, A.C., Phillips, C., Kazanina, N., Poeppel, D., 2010. The linguistic processes underlying the P600. Lang. Cognit. Process. 25 (2), 149–188.

Gu, L., Zhang, Z., 2017. Exploring potential electrophysiological biomarkers in mild cognitive impairment: a systematic review and meta-analysis of event-related potential studies. J. Alzheimer's Dis. 58 (4), 1283–1292.

Gu, L., Chen, J., Gao, L., Shu, H., Wang, Z., Liu, D., et al., 2018. Cognitive reserve modulates attention processes in healthy elderly and amnestic mild cognitive impairment: An event-related potential study. Clin. Neurophysiol. 129 (1), 198–207.

Guest, F.L., Rahmoune, H., Guest, P.C., 2022. Early Diagnosis and Targeted Treatment Strategy for Improved Therapeutic Outcomes in Alzheimer's Disease. In: Guest PC, editor. Reviews on New Drug Targets in Age-Related Disorders [Internet]. Cham: Springer International Publishing; 2020 [cited 2022 Nov 27]. p. 175–91. (Advances in Experimental Medicine and Biology). Available from: https://doi.org/10.1007/978-3-030-42667-5_8.

Habeck, C., Hilton, H.J., Zarahn, E., Flynn, J., Moeller, J., Stern, Y., 2003. Relation of cognitive reserve and task performance to expression of regional covariance networks in an event-related fMRI study of nonverbal memory. Neuroimage 20 (3), 1723–1733.

Harding, G.F.A., Wright, C.E., Orwin, A., 1985. Primary presenile dementia: the use of the visual evoked potential as a diagnostic indicator. Br. J. Psychiatry 147 (5), 532–539.

Hasanzadeh, F., Habeck, C., Gazes, Y., Stern, Y., 2025. A neural implementation of cognitive reserve: Insights from a longitudinal fMRI study of set-switching in aging. Neurobiol. Aging 145, 76–83.

Hedges, D., Janis, R., Mickelson, S., Keith, C., Bennett, D., Brown, B.L., 2016. P300 amplitude in Alzheimer's disease: a meta-analysis and meta-regression. Clin. EEG Neurosci. 47 (1), 48–55.

Hendriksen, H.M.A., de Rijke, T.J., Fruijtier, A., van de Giessen, E., van Harten, A.C., van Leeuwenstijn-Koopman, M.S.S.A., et al., 2024. Amyloid PET disclosure in subjective cognitive decline: Patient experiences over time. Alzheimers Dement. 20 (9), 6556–6565.

Hong, Y.J., Ho, S., Jeong, J.H., Park, K.H., Kim, S., Wang, M.J., et al., 2023. Impacts of baseline biomarkers on cognitive trajectories in subjective cognitive decline: the CoSCo prospective cohort study. Alzheimers Res. Ther. 15 (1), 132.

Horvath, A., Szucs, A., Csukly, G., Sakovics, A., Stefanics, G., Kamondi, A., 2018. EEG and ERP biomarkers of Alzheimer's disease: a critical review. Front. Biosci. (landmark Edition). 1 (23), 183–220.

Hull, J., Harsh, J., 2001. P300 and sleep-related positive waveforms (P220, P450, and P900) have different determinants. J. Sleep Res. 10 (1), 9–17.

Ieracitano, C., Mammone, N., Hussain, A., Morabito, F.C., 2020. A novel multi-modal machine learning based approach for automatic classification of EEG recordings in dementia. Neural Netw. 1 (123), 176–190.

Jack, C.R., Bennett, D.A., Blennow, K., Carrillo, M.C., Feldman, H.H., Frisoni, G.B., et al., 2016. A/T/N: An unbiased descriptive classification scheme for Alzheimer disease biomarkers. Neurology 87 (5), 539–547.

Jae, K.M., Youn, Y.C., Paik, J., 2023. Deep learning-based EEG analysis to classify normal, mild cognitive impairment, and dementia: Algorithms and dataset. Neuroimage 15 (272), 120054.

Javitt, D.C., Martinez, A., Sehatpour, P., Beloborodova, A., Habeck, C., Gazes, Y., et al., 2023. Disruption of early visual processing in amyloid-positive healthy individuals and mild cognitive impairment. Alzheimers Res. Ther. 15 (1), 42.

Jessen, F., Amariglio, R.E., van Boxtel, M., Breteler, M., Ceccaldi, M., Chételat, G., et al., 2014. A conceptual framework for research on subjective cognitive decline in preclinical Alzheimer's disease. Alzheimer's & Dementia. 10 (6), 844–852.

Jessen, F., Amariglio, R.E., van Boxtel, M., Breteler, M., Ceccaldi, M., Chételat, G., et al., 2014. A conceptual framework for research on subjective cognitive decline in preclinical Alzheimer's disease. Alzheimers Dement. 10 (6), 844–852.

Jessen, F., Amariglio, R.E., Buckley, R.F., van der Flier, W.M., Han, Y., Molinuevo, J.L., et al., 2020. The characterisation of subjective cognitive decline. Lancet Neurol. 19 (3), 271–278.

Jiang, S., Qu, C., Wang, F., Liu, Y., Qiao, Z., Qiu, X., et al., 2015. Using event-related potential P300 as an electrophysiological marker for differential diagnosis and to predict the progression of mild cognitive impairment: a meta-analysis. Neurol. Sci. 36 (7), 1105–1112.

Karamacoska, D., Barry, R.J., De Blasio, F.M., Steiner, G.Z., 2019. EEG-ERP dynamics in a visual continuous performance test. Int. J. Psychophysiol. 1 (146), 249–260.

Katayama, O., Stern, Y., Habeck, C., Coors, A., Lee, S., Harada, K., et al., 2024. Detection of neurophysiological markers of cognitive reserve: an EEG study. Front. Aging Neurosci. 16, 1401818.

Kim, N.H., Yang, D.W., Choi, S.H., Kang, S.W., 2021. Machine Learning to Predict Brain Amyloid Pathology in Pre-dementia Alzheimer's Disease Using QEEG Features and Genetic Algorithm Heuristic. Front Comput Neurosci. 202115. Available from: https://www.frontiersin.org/journals/computational-neuroscience/articles/10.3389/fncom.2021.755499/full.

Kimiskidis, V.K., Papaliagkas, V.T., 2012. Event-related potentials for the diagnosis of mild cognitive impairment and Alzheimer's disease. Expert Opin. Med. Diagn. 6 (1), 15–26.

Knopman, D.S., 2024. For a dementia diagnosis, clinical acumen must precede biomarkers. Lancet Neurol. 23 (3), 225–226.

Koenig, T., Prichep, L., Lehmann, D., Sosa, P.V., Braeker, E., Kleinlogel, H., et al., 2002. Millisecond by millisecond, year by year: normative EEG microstates and developmental stages. Neuroimage 16 (1), 41–48.

Kolev, V., Yordanova, J., Basar-Eroglu, C., Basar, E., 2002. Age effects on visual EEG responses reveal distinct frontal alpha networks. Clin. Neurophysiol. 113 (6), 901–910.

Krasodomska, K., Lubiński, W., Potemkowski, A., Honczarenko, K., 2010. Pattern electroretinogram (PERG) and pattern visual evoked potential (PVEP) in the early stages of Alzheimer's disease. Doc. Ophthalmol. 121 (2), 111–121.

Lassi, M., Fabbiani, C., Mazzeo, S., Burali, R., Vergani, A.A., Giacomucci, G., et al., 2023. Degradation of EEG microstates patterns in subjective cognitive decline and mild cognitive impairment: early biomarkers along the Alzheimer's Disease continuum? Neuroimage Clin. 38, 103407.

Lavanga, M., Stumme, J., Yalcinkaya, B.H., Fousek, J., Jockwitz, C., Sheheitli, H., et al., 2023. The virtual aging brain: a model-driven explanation for cognitive decline in older subjects [Internet]. bioRxiv; 2022 [cited 2023 Jul 13]. p. 2022.02.17.480902. Available from: https://www.biorxiv.org/content/10.1101/2022.02.17.480902v2.

Leckey, M., Federmeier, K.D., 2020. The P3b and P600(s): Positive contributions to language comprehension. Psychophysiology 57 (7), e13351.

Lipp, I., Benedek, M., Fink, A., Koschutnig, K., Reishofer, G., Bergner, S., et al., 2012. Investigating neural efficiency in the visuo-spatial domain: An fmri Study. PLoS One 7 (12), e51316.

Liu, S., Luo, X., Chong, J.S.X., Jiaerken, Y., Youn, S.H., Zhang, M., et al., 2024. Brain structure, amyloid, and behavioral features for predicting clinical progression in subjective cognitive decline. Hum. Brain Mapp. 45 (10), e26765.

Livingston, G., Huntley, J., Sommerlad, A., Ames, D., Ballard, C., Banerjee, S., et al., 2020. Dementia prevention, intervention, and care: 2020 report of the Lancet Commission. Lancet 396 (10248), 413–446.

Luck, S.J., Heinze, H.J., Mangun, G.R., Hillyard, S.A., 1990. Visual event-related potentials index focused attention within bilateral stimulus arrays. II. Functional

dissociation of P1 and N1 components. Electroencephalogr. Clin. Neurophysiol. 75 (6), 528–542.
Luck, S.J., Hillyard, S.A., Mouloua, M., Woldorff, M.G., Clark, V.P., Hawkins, H.L., 1994. Effects of spatial cuing on luminance detectability: Psychophysical and electrophysiological evidence for early selection. J. Exp. Psychol. Hum. Percept. Perform. 20, 887–904.
Mangun, G.R., 1995. Neural mechanisms of visual selective attention. Psychophysiology 32 (1), 4–18.
Mangun, G.R., Hillyard, S.A., 1991. Modulations of sensory-evoked brain potentials indicate changes in perceptual processing during visual-spatial priming. J. Exp. Psychol. Hum. Percept. Perform. 17 (4), 1057–1074.
Matchett, B.J., Grinberg, L.T., Theofilas, P., Murray, M.E., 2021. The mechanistic link between selective vulnerability of the locus coeruleus and neurodegeneration in Alzheimer's disease. Acta Neuropathol. 141 (5), 631–650.
Mather, M., Harley, C.W., 2016. The locus coeruleus: essential for maintaining cognitive function and the aging brain. Trends Cogn. Sci. 20 (3), 214–226.
Mazure, C.M., Swendsen, J., 2016. Sex differences in Alzheimer's disease and other dementias. Lancet Neurol. 15 (5), 451–452.
Mazzeo, S., Lassi, M., Padiglioni, S., Vergani, A.A., Moschini, V., Scarpino, M., et al., 2024. Towards the development of a management protocol for Subjective Cognitive Decline: insights from a cross-sectional and longitudinal analyses of multimodal data from a memory clinic [Internet]. medRxiv;p. 2024.10.15.24315516. Available from: https://www.medrxiv.org/content/10.1101/2024.10.15.24315516v2.
Mazzeo, S., Lassi, M., Padiglioni, S., Vergani, A.A., Moschini, V., Scarpino, M., et al., 2023. PRedicting the EVolution of SubjectIvE Cognitive Decline to Alzheimer's Disease With machine learning: the PREVIEW study protocol. BMC Neurol. 23 (1), 300.
Mazzeo, S., Ingannato, A., Giacomucci, G., Manganelli, A., Moschini, V., Balestrini, J., et al., 2024. Plasma neurofilament light chain predicts Alzheimer's disease in patients with subjective cognitive decline and mild cognitive impairment: a cross-sectional and longitudinal study. Eur. J. Neurol. 31 (1), e16089.
McKhann, G.M., Knopman, D.S., Chertkow, H., Hyman, B.T., Jack, C.R., Kawas, C.H., et al., 2011. The diagnosis of dementia due to Alzheimer's disease: Recommendations from the National Institute on Aging-Alzheimer's Association workgroups on diagnostic guidelines for Alzheimer's disease. Alzheimer's Dementia 7 (3), 263–269.
Meixner, J.B., Labkovsky, E., Peter Rosenfeld, J., Winograd, M., Sokolovsky, A., Weishaar, J., et al., 2013. P900: a putative novel ERP component that indexes countermeasure use in the p300-based concealed information test. Appl. Psychophysiol. Biofeedback 38 (2), 121–132.
Mengel, D., Soter, E., Ott, J.M., Wacker, M., Leyva, A., Peters, O., et al., 2024. Blood biomarkers confirm subjective cognitive decline (SCD) as a distinct molecular and clinical stage within the NIA-AA framework of Alzheimer's disease [Internet]. medRxiv; p. 2024.07.10.24310205. Available from: https://www.medrxiv.org/content/10.1101/2024.07.10.24310205v1.
Mevel, K., Chételat, G., Eustache, F., Desgranges, B., 2011. The default mode network in healthy aging and Alzheimer's Disease. Int. J. Alzheimer's Dis. 2011 (1), 535816.
Mielke, M.M., 2018. Sex and gender differences in Alzheimer's Disease dementia. Psychiatr. times 35 (11), 14–17.
Monteverdi, A., Palesi, F., Schirner, M., Argentino, F., Merante, M., Redolfi, A., et al., 2023. Virtual brain simulations reveal network-specific parameters in neurodegenerative dementias. Front. Aging Neurosci., 2023, 15. Available from: https://www.frontiersin.org/journals/aging-neuroscience/articles/10.3389/fnagi.2023.1204134/full.
Monteverdi, A., Palesi, F., Costa, A., Vitali, P., Pichiecchio, A., Cotta Ramusino, M., et al., 2022. Subject-specific features of excitation/inhibition profiles in neurodegenerative diseases. Aug 5 [cited 2025 Feb 11];14. Available from: Front Aging Neurosci. https://www.frontiersin.org/journals/aging-neuroscience/articles/10.3389/fnagi.2022.868342/full.
Morrison, C., Rabipour, S., Knoefel, F., Sheppard, C., Taler, V., 2018. Auditory Event-related Potentials in Mild Cognitive Impairment and Alzheimer's Disease. Curr. Alzheimer Res. 15 (8), 702–715.
Morrison, C., Rabipour, S., Taler, V., Sheppard, C., Knoefel, F., 2019. Visual event-related potentials in mild cognitive impairment and Alzheimer's disease: a literature review. Curr. Alzheimer Res. 16 (1), 67–89.
Mulert, C., Pogarell, O., Juckel, G., Rujescu, D., Giegling, I., Rupp, D., et al., 2004. The neural basis of the P300 potential. Eur. Arch. Psychiatry Clin. Neurosci. 254 (3), 190–198.
Oakley, D., Joffe, D., Palermo, F., Spada, M., Yathiraj, S., 2025. The P200 ERP response in mild cognitive impairment and the aging population. Clin. EEG Neurosci. 15500594241310533.
Olichney, J.M., Taylor, J.R., Gatherwright, J., Salmon, D.P., Bressler, A.J., Kutas, M., et al., 2008. Patients with MCI and N400 or P600 abnormalities are at very high risk for conversion to dementia. Neurology 70 (19_part_2), 1763–1770.
Olichney, J.M., Pak, J., Salmon, D.P., Yang, J.C., Gahagan, T., Nowacki, R., et al., 2013. Abnormal P600 word repetition effect in elderly persons with preclinical Alzheimer's disease. Cogn. Neurosci. 4 (3–4), 143–151.
Paitel, E.R., Samii, M.R., Nielson, K.A., 2021. A systematic review of cognitive event-related potentials in mild cognitive impairment and Alzheimer's disease. Behav. Brain Res. 1 (396), 112904.
Parra, M., Ascencio, L., Urquina, H., Manes, F., Ibanez, A., 2012. P300 and neuropsychological assessment in mild cognitive impairment and alzheimer dementia. Front Neurol. 2012 ;3. Available from: https://www.frontiersin.org/journals/neurology/articles/10.3389/fneur.2012.00172/full.
Perrotin, A., Mormino, E.C., Madison, C.M., Hayenga, A.O., Jagust, W.J., 2012. Subjective cognition and amyloid deposition imaging: a Pittsburgh compound b positron emission tomography study in normal elderly individuals. Arch. Neurol. 69 (2), 223–229.
Polich, J., Ehlers, C.L., Otis, S., Mandell, A.J., Bloom, F.E., 1986. P300 latency reflects the degree of cognitive decline in dementing illness. Electroencephalogr. Clin. Neurophysiol. 63 (2), 138–144.
Pollock, V.E., Schneider, L.S., Chui, H.C., Henderson, V., Zemansky, M., Sloane, R.B., 1989. Visual evoked potentials in dementia: A meta-analysis and empirical study of Alzheimer's disease patients. Biol. Psychiatry 25 (8), 1003–1013.
Pukelsheim, F., 1994. The three sigma rule. Am. Stat. 48 (2), 88–91.
Quinzi, F., Berchicci, M., Bianco, V., Di Filippo, G., Perri, R.L., Di Russo, F., 2020. The role of cognitive reserve on prefrontal and premotor cortical activity in visuo-motor response tasks in healthy old adults. Neurobiol. Aging 94, 185–195.
Rabin, L.A., Smart, C.M., Crane, P.K., Amariglio, R.E., Berman, L.M., Boada, M., et al., 2015. Subjective cognitive decline in older adults: an overview of self-report measures used across 19 international research studies. J. Alzheimer's Dis. 48 (s1), S63–S86.
Ramchandran, K., Zeien, E., Andreasen, N.C., 2019. Distributed neural efficiency: Intelligence and age modulate adaptive allocation of resources in the brain. Trends Neurosci. Educ. 1 (15), 48–61.
Rosenfeld, J.P., Labkovsky, E., 2010. New P300-based protocol to detect concealed information: Resistance to mental countermeasures against only half the irrelevant stimuli and a possible ERP indicator of countermeasures. Psychophysiology 47 (6), 1002–1010.
Rossini, P.M., Miraglia, F., Vecchio, F., 2022. Early dementia diagnosis, MCI-to-dementia risk prediction, and the role of machine learning methods for feature extraction from integrated biomarkers, in particular for EEG signal analysis. Alzheimer's & Dementia. 18 (12), 2699–2706.
Rutkowski, T.M., Abe, M.S., Komendzinski, T., Sugimoto, H., Narebski, S., 2023. Otake-Matsuura M. Machine learning approach for early onset dementia neurobiomarker using EEG network topology features. Front Hum Neurosci. 2023 Jun 16 [cited 2024 Jul 11];17. Available from: https://www.frontiersin.org/journals/human-neuroscience/articles/10.3389/fnhum.2023.1155194/full.
Sabri, O., Sabbagh, M.N., Seibyl, J., Barthel, H., Akatsu, H., Ouchi, Y., et al., 2015. Florbetaben PET imaging to detect amyloid beta plaques in Alzheimer's disease: phase 3 study. Alzheimers Dement. 11 (8), 964–974.
Saito, H., Yamazaki, H., Matsuoka, H., Matsumoto, K., Numachi, Y., Yoshida, S., et al., 2001. Visual event-related potential in mild dementia of the Alzheimer's type. Psychiatry Clin. Neurosci. 55 (4), 365–371.
Sassenhagen, J., Schlesewsky, M., Bornkessel-Schlesewsky, I., 2014. The P600-as-P3 hypothesis revisited: Single-trial analyses reveal that the late EEG positivity following linguistically deviant material is reaction time aligned. Brain Lang. 1 (137), 29–39.
Sibilano, E., Brunetti, A., Buongiorno, D., Lassi, M., Grippo, A., Bessi, V., et al., 2023. An attention-based deep learning approach for the classification of subjective cognitive decline and mild cognitive impairment using resting-state EEG. J. Neural Eng. 20 (1), 016048.
Sibilano, E., Buongiorno, D., Lassi, M., Grippo, A., Bessi, V., Sorbi, S., et al., 2024. Understanding the role of self-attention in a transformer model for the discrimination of SCD from MCI using resting-state EEG. IEEE J. Biomed. Health Inform. 28 (6), 3422–3433.
Siems, M., Pape, A.A., Hipp, J.F., Siegel, M., 2016. Measuring the cortical correlation structure of spontaneous oscillatory activity with EEG and MEG. Neuroimage 1 (129), 345–355.
Slot, R.E.R., Sikkes, S.A.M., Berkhof, J., Brodaty, H., Buckley, R., Cavedo, E., et al., 2019. Subjective cognitive decline and rates of incident Alzheimer's disease and non–Alzheimer's disease dementia. Alzheimer's & Dementia. 15 (3), 465–476.
Smailovic, U., Koenig, T., Kåreholt, I., Andersson, T., Kramberger, M.G., Winblad, B., et al., 2018. Quantitative EEG power and synchronization correlate with Alzheimer's disease CSF biomarkers. Neurobiol. Aging 63, 88–95.
Spearman, C., 1961. The Proof and Measurement of Association Between Two Things. East Norwalk, CT, US: Appleton-Century-Crofts. 45 p. (Studies in individual differences: The search for intelligence).
Speer, M.E., Soldan, A., 2015. Cognitive reserve modulates ERPs associated with verbal working memory in healthy younger and older adults. Neurobiol. Aging 36 (3), 1424–1434.
Sperling, R.A., Aisen, P.S., Beckett, L.A., Bennett, D.A., Craft, S., Fagan, A.M., et al., 2011. Toward defining the preclinical stages of Alzheimer's disease: Recommendations from the National Institute on Aging-Alzheimer's Association workgroups on diagnostic guidelines for Alzheimer's disease. Alzheimer's & Dementia. 7 (3), 280–292.
Stern, Y., 2006. Cognitive reserve and alzheimer disease. Alzheimer Dis. Assoc. Disord. 20 (2), 112.
Stern, Y., 2009. Cognitive reserve. Neuropsychologia 47 (10), 2015–2028.
Stern, Y., Zarahn, E., Hilton, H.J., Flynn, J., DeLaPaz, R., Rakitin, B., 2003. Exploring the neural basis of cognitive reserve. J. Clin. Exp. Neuropsychol. 25 (5), 691–701.
Stern, Y., Albert, M., Barnes, C.A., Cabeza, R., Pascual-Leone, A., Rapp, P.R., 2023. A framework for concepts of reserve and resilience in aging. Neurobiol. Aging 1 (124), 100–103.
Stikic, M., Johnson, R.R., Levendowski, D.J., Popovic, D.P., Olmstead, R.E., Berka, C., 2011. EEG-derived estimators of present and future cognitive performance. Front. Hum. Neurosci. 5, 70.
Sundermann, E.E., Maki, P., Biegon, A., Lipton, R.B., Mielke, M.M., Machulda, M., et al., 2019. Sex-specific norms for verbal memory tests may improve diagnostic accuracy of amnestic MCI. Neurology 93 (20), e1881–e1889.

Tan, A., Hu, L., Tu, Y., Chen, R., Hung, Y.S., Zhang, Z., 2016. N1 magnitude of auditory evoked potentials and spontaneous functional connectivity between bilateral heschl's gyrus are coupled at interindividual level. Brain Connect. 6 (6), 496–504.
Theofilas, P., Ehrenberg, A.J., Dunlop, S., Di Lorenzo Alho, A.T., Nguy, A., Leite, R.E.P., et al., 2017. Locus coeruleus volume and cell population changes during Alzheimer's disease progression: A stereological study in human postmortem brains with potential implication for early-stage biomarker discovery. Alzheimer's & Dementia. 13 (3), 236–246.
Tomlinson, B.E., Irving, D., Blessed, G., 1981. Cell loss in the locus coeruleus in senile dementia of Alzheimer type. J. Neurol. Sci. 49 (3), 419–428.
Valles-Salgado, M., Gil-Moreno, M.J., Curiel Cid, R.E., Delgado-Álvarez, A., Ortega-Madueño, I., Delgado-Alonso, C., et al., 2024. Detection of cerebrospinal fluid biomarkers changes of Alzheimer's disease using a cognitive stress test in persons with subjective cognitive decline and mild cognitive impairment. Front. Psychol. 15, 1373541.
van Deursen, J.A., Vuurman, E.F.P.M., Smits, L.L., Verhey, F.R.J., Riedel, W.J., 2009. Response speed, contingent negative variation and P300 in Alzheimer's disease and MCI. Brain Cogn. 69 (3), 592–599.
van Dyck, C.H., Swanson, C.J., Aisen, P., Bateman, R.J., Chen, C., Gee, M., et al., 2023. Lecanemab in Early Alzheimer's disease. N. Engl. J. Med. 388 (1), 9–21.
van Harten, A.C., Visser, P.J., Pijnenburg, Y.A.L., Teunissen, C.E., Blankenstein, M.A., Scheltens, P., et al., 2013. Cerebrospinal fluid Aβ42 is the best predictor of clinical progression in patients with subjective complaints. Alzheimer's & Dementia. 9 (5), 481–487.
Vockert, N., Machts, J., Kleineidam, L., Nemali, A., Incesoy, E.I., Bernal, J., et al., 2024. Cognitive reserve against Alzheimer's pathology is linked to brain activity during memory formation. Nat. Commun. 15 (1), 9815.
Wang, J., Li, C., Yu, X., Zhao, Y., Shan, E., Xing, Y., et al., 2024. Effect of emotional stimulus on response inhibition in people with mild cognitive impairment: an event-related potential study. Apr 30 [cited 2024 Jul 10];18. Available from: Front. Neurosci. https://www.frontiersin.org/journals/neuroscience/articles/10.3389/fnins.2024.1357435/full.
Wang, H.E., Triebkorn, P., Breyton, M., Dollomaja, B., Lemarechal, J.D., Petkoski, S., et al., 2024. Virtual brain twins: from basic neuroscience to clinical use. Natl. Sci. Rev. 11 (5) nwae079.
Waninger, S., Berka, C., Meghdadi, A., Karic, M.S., Stevens, K., Aguero, C., et al., 2018. Event-related potentials during sustained attention and memory tasks: Utility as biomarkers for mild cognitive impairment. Alzheimer's & Dementia: Diagnosis, Assessment & Disease Monit. 1 (10), 452–460.
Woldorff, M.G., Fox, P.T., Matzke, M., Lancaster, J.I., Veeraswamy, S., Zamarripa, F., et al., 1997. Retinotopic organization of early visual spatial attention effects as revealed by PET and ERPs. Hum. Brain Mapp. 5 (4), 280–286.
Xia, J., Kutas, M., Salmon, D.P., Stoermann, A.M., Rigatuso, S.N., Tomaszewski Farias, S. E., et al., 2024. Memory-related brain potentials for visual objects in early AD show impairment and compensatory mechanisms. Cereb. Cortex 34 (10) bhae398.
Xiao, S., Li, Y., Liu, M., Li, Y., 2022. Electrophysiological evidence of impaired cognitive reappraisal in amnestic mild cognitive impairment: An event-related potential study. Behav. Brain Res. 3 (427), 113800.
Young, A.L., Marinescu, R.V., Oxtoby, N.P., Bocchetta, M., Yong, K., Firth, N.C., et al., 2018. Uncovering the heterogeneity and temporal complexity of neurodegenerative diseases with Subtype and Stage Inference. Nat. Commun. 9 (1), 4273.
Zhang, J., Xia, J., Liu, X., Olichney, J., 2023. Machine learning on visibility graph features discriminates the cognitive event-related potentials of patients with early alzheimer's disease from healthy aging. Brain Sci. 13 (5), 770.